

Attn: J.T. Greaves

*see Pocket-1
for qual. sheets*
WTSD-TME-030
DRAFT

To: J. Greaves, WMEG
From: F.R. Cook, On-site Rep., NRC

Packing Emplacement Development Tests

Joseph M. Markowitz
Matt J. Lerach

WM Record File 101
WM Project 10
Docket No. _____
PDR
LPDR

APRIL 1984

Distribution:
J. Greaves
(Return to WM, 623-SS) C²

WM DOCKET CONTROL
CENTER
84 JUL 16 AM 1:47

prepared for
Rockwell Hanford Operations
Energy Systems Group in Support of the
Basalt Waste Isolation Project
Subcontract Number CPFF-880

WESTINGHOUSE ELECTRIC CORPORATION
Waste Technology Services Division
P.O. Box 10864
Pittsburgh, Pennsylvania 15236

8407240601 840430
PDR WASTE PDR
WM-10

00884

DISCLAIMER

This report was prepared as an account of work sponsored by an agency of the United States Government. Neither the United States Government nor any agency thereof, nor any of their employees, makes any warranty, express or implied, or assumes any legal liability or responsibility for the accuracy, completeness, or usefulness of any information, apparatus, product or process disclosed, or represents that its use would not infringe privately owned rights. References herein to any specific commercial product, process, or service by trade name, trademark, manufacturer, or otherwise, does not necessarily constitute or imply its endorsement, recommendation, or favoring by the United States Government or any agency thereof. The views and opinions of authors expressed herein do not necessarily state or reflect those of the United States Government or any agency thereof.

APPROVED

_____ W.M. George, Jr.
_____ Director
_____ 1954
_____ 1954
_____ 1954
_____ 1954
_____ 1954
_____ 1954

see folder for
the cover sheet
titled Packing Emplacement
Development Tests.
4/84

101
Pocket 1

WTSD-TME-030
DRAFT

PACKING EMPLACEMENT DEVELOPMENT TESTS

Joseph M. Markowitz and Matthew J. Lerach

ABSTRACT

The pneumatic emplacement of a crushed basalt and bentonite packing mixture (3:1 ratio) into a simulated long horizontal borehole containing several waste package mockups has been studied using a dilute phase delivery system. Reasonably homogeneous packing was accomplished at a density of 1.56 g/cc, or 58% theoretical. Ranges of practical operating parameters were developed. Recommendations are made for further development and upgrading of the equipment and operations, with the object of approaching more closely to the nominal target density of 70% theoretical.

ACKNOWLEDGMENTS

The work described herein was performed as part of Tasks 1-7 of Rockwell International Subcontract CPFF-880. The Westinghouse Project Manager was Dr. James R. Schomhorst and the Rockwell Project Manager was Mr. William J. Anderson. In addition to the authors, other contributors to this project were

J. Burkett
T. Dolovacki
G. V. B. Hall
R. F. Kehrman
G. R. Kilp
F. Knight
D. H. Kurasch
R. Pikuiski
R. Schmidt

The authors are grateful for their assistance, advice and helpful consultations.

TABLE OF CONTENTS

	Page
1. INTRODUCTION	1
2. EXPERIMENT	3
2.1 Apparatus	3
2.2 Materials	12
2.2.1 Characterization and Analysis	12
2.2.2 Basalt	14
2.2.3 Bentonite	15
2.2.4 Packaging	15
2.3 Operations	17
2.3.1 Preliminaries	17
2.3.2 Conduct of Tests	17
2.3.3 Post-test Activities	21
3. RESULTS AND DISCUSSION	22
3.1 Overview	22
3.2 Data	22
3.2.1 System Parameters	22
3.2.2 Density	27
3.2.3 Mineral Homogeneity	28
3.2.4 Interactions	33
3.3 General Observations	33
4. CONCLUSIONS	35
5. RECOMMENDATIONS	36
6. REFERENCES	38

TABLE OF CONTENTS (Continued)

	Page
7. APPENDIXES	39
Appendix A Apparatus	40
A.1 Test Section	40
A.2 Feed System	44
A.3 Exhaust System	46
A.4 Instrumentation	46
Appendix B Analysis of Packing for Basalt Concentration	56
B.1 Material and Equipment	57
B.2 Preparation	58
B.3 Subsample Preparation	59
B.4 Dilution Procedure	60
B.5 Filtration	61
B.6 Drying and Weighing	62
B.7 Calculations	63
Appendix C Data and Analysis	65
C.1 Methodology	66
C.2 Density	66
C.3 Mineral Homogeneity	77
C.4 Interactions	84
Appendix D Sample Data Sheets	85
Appendix E Listing and Sample Output of Computer Program HIERARC2	90

LIST OF FIGURES

<u>Figure No.</u>	<u>Title</u>	<u>Page</u>
1	Assembled Simulator, Rear	4
2	Assembled Simulator, Front	5
3	Hoppers	7
4	System Layout	8
5	Load Cell	9
6	Load Cell Instrumentation	10
7	Instrumentation and Controls	11
8	Sample Cylinder	13
9	Tap Densities	16
10	Wedge Nozzles, Test 3	25
11	Wedge Nozzles, Test 4	26
12	Density Distribution, Run 3	29
13	Density Distribution, Run 4	30
14	Basalt Concentration Distribution, Run 3	31
15	Basalt Concentration Distribution, Run 4	32
16	Bentonite Hopper Feed Screw Calibration	48
17	Basalt Hopper Feed Screw Calibration	49
18	Resolution of Variances	68

The overall objectives of this program are to:

- o Determine if a bentonite and basalt mixture can be pneumatically installed as a packing, in a test configuration dimensionally representative of the NWRB conceptual design, to achieve a reasonably homogeneous, installed density equal to or greater than a target value currently specified to be 70% of the theoretical solid density of the packing materials. This value is expected to be lower when additional experimental data become available.
- o Characterize key process parameters used to achieve these results.

More specific objectives were established to meet these overall objectives:

- o Design and build a test apparatus that simulates the emplacement hole-canister-packing interface, the packing installation equipment, and the packing method included in the NWRB conceptual design.
- o Obtain and use actual packing materials.
- o Provide the following data:
 - starting packing particle size and preparation
 - pneumatic system settings, operating parameters, and performance
 - annulus fill rate
 - installed density (average and local)
 - installed homogeneity (average and local)

This report discusses the test apparatus and the materials which were combined and emplaced to form the packing. Details of the apparatus and its assembly are found in Appendix A. Test operations are described, and results are tabulated and discussed. Again, details of the analysis and raw data tables and summaries are provided in an appendix. General observations on the test operation are presented, followed by conclusions and recommendations.

2 EXPERIMENT

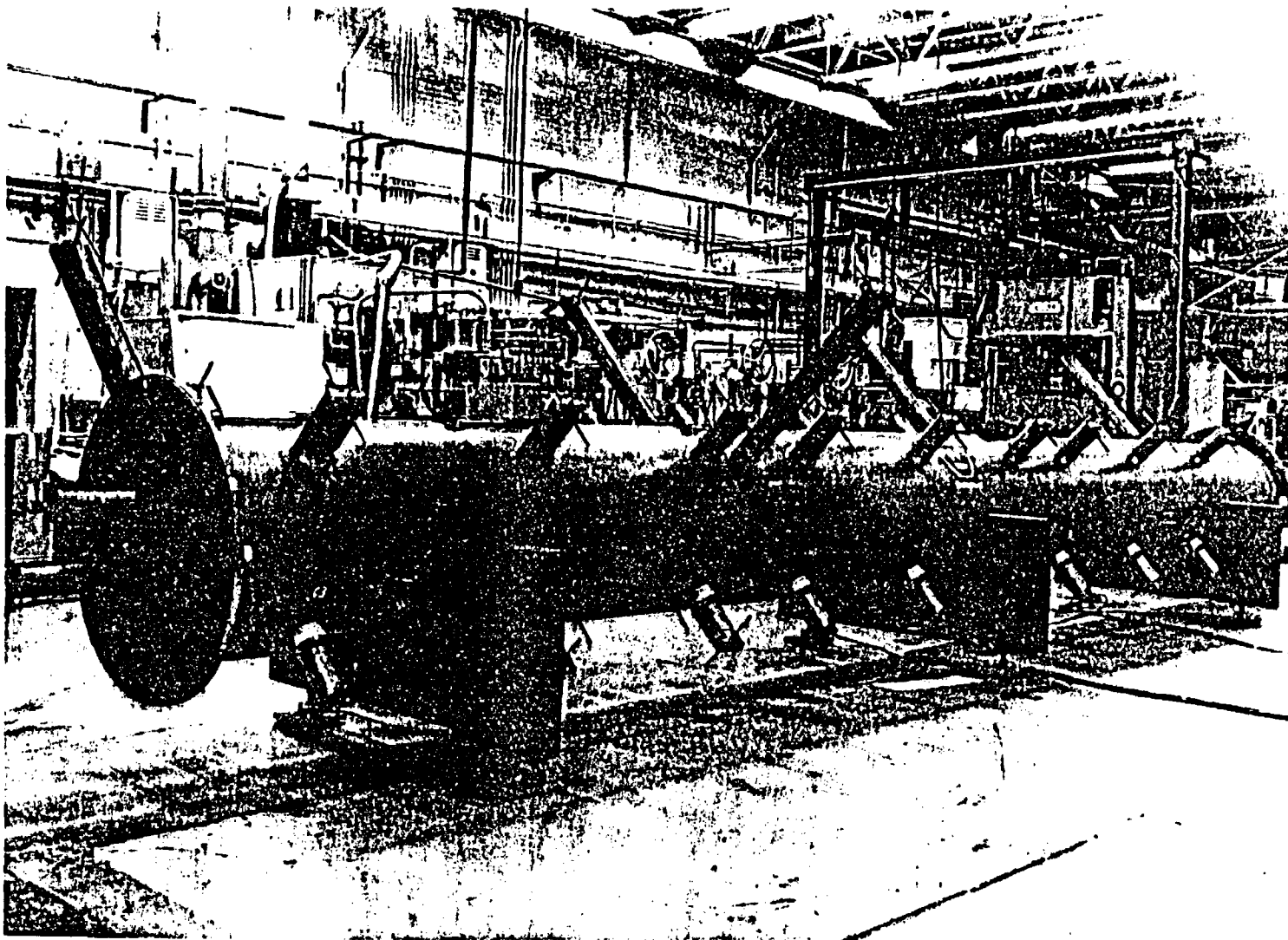
2.1 APPARATUS

The experimental apparatus is comprised of four major elements:

- (1) A test section, essentially a borehole simulator;
- (2) A feed section, including feed hoppers and transport tubing;
- (3) An exhaust section, with a pump to produce the required vacuum to drive material transport.
- (4) Appropriate instrumentation to follow the deposition rate of the packing, air velocity, pressures at key points in the system, and feed rates of the solids.

Details of the apparatus and its construction, along with engineering drawings, are presented in Appendix A. The following paragraphs summarize each of the elements above.

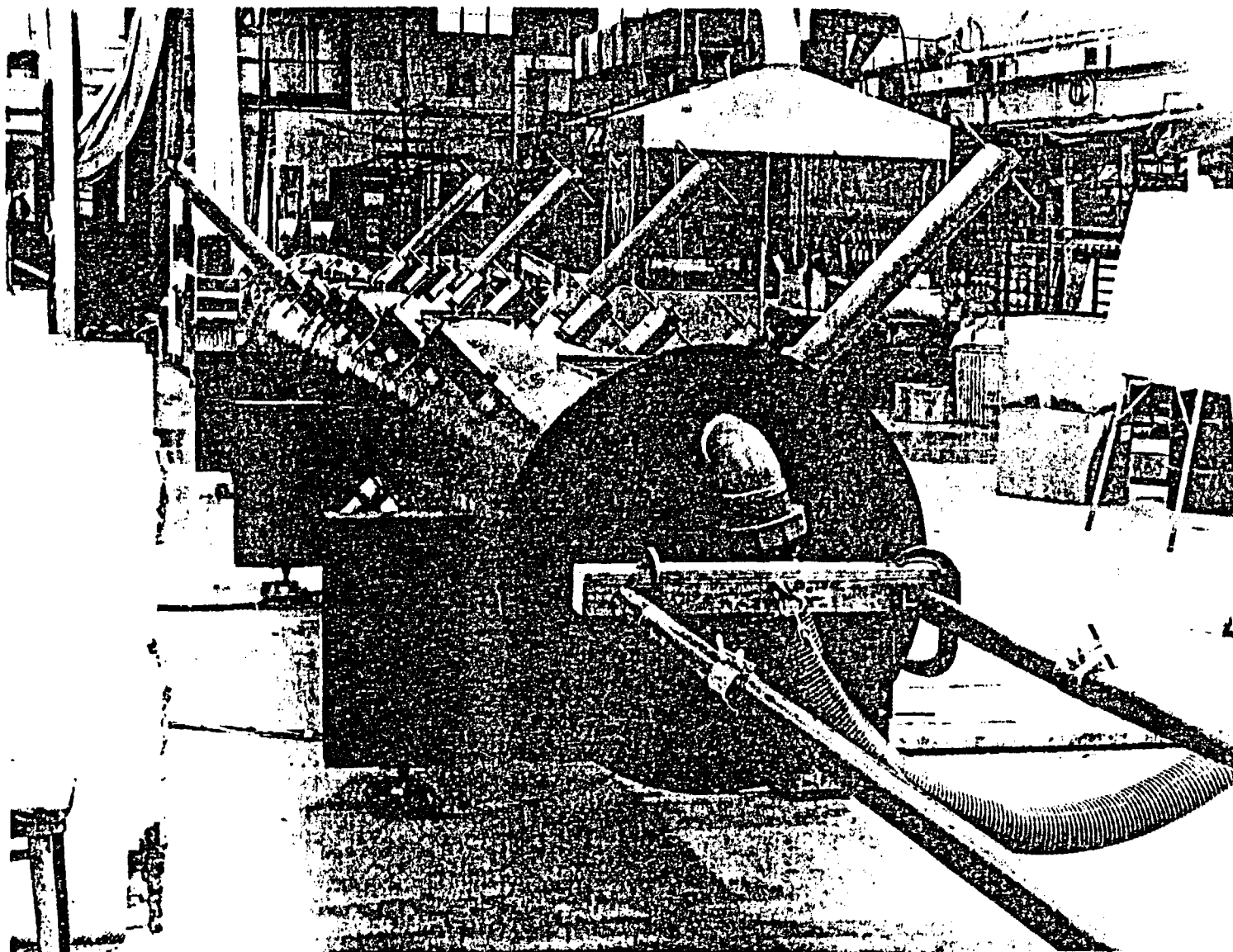
The test section, or borehole simulator, shown in Figures 1 and 2, is a cylinder about a meter in diameter, and about eight and a half meters long, within which are centered three waste package mockups, evenly placed along the length. Forty-one sampling ports are distributed about the simulator circumference, and there are two in one of the end plates. Five of the circumferential samplers core across the full simulator diameter, and the remaining 36 core through the annulus around the waste package mockups. One end plate, opposite that containing the sampling ports, contains openings for admitting packing feed pipes and an exhaust port for connection with the exhaust system. The object of the experiment is to fill this test section with packing to the target density, with acceptable homogeneity of the packing components.



4

Figure 1. Rear View of Assembled Simulator, Showing Sampling Cylinders "Out" Position. Note the two end cylinders.

HTSD-THE-030
DRAFT



5

Figure 2. Front View of Assembled Simulator, Showing Yoke Used to Extract Feed Pipes as Simulator Fills. Note cable attached to yoke.

HTSD-THE-030
DRAFT

Horizontal transfer of aggregate materials was performed pneumatically using dilute phase procedures and equipment, because the long delivery span and relatively large particle size material, especially the basalt, imposed a requirement for relative immunity to saltation and consequent blockage. In principle, the dilute phase mode, with its provision for transfer with only a small fraction of the transfer piping volume filled at any one time (voidage in excess of 90%), provides this immunity (Reference 3). Accordingly, the feed system consists of a pair of 100 cu. ft. capacity hoppers (more than sufficient for the necessary combined bulk of the components; see Figure 3), a metering system to add solids from the hoppers to the air stream at the desired rate in the specified proportions, and a delivery line to carry the pneumatically entrained material to the simulator. This delivery line breaks into two at a vee-splitter a few meters downstream of the feed hoppers, creating parallel delivery lines, one for each side of the simulator. These delivery lines terminate in a pair of feed pipes within the simulator, which can be withdrawn as the simulator fills. Part of the connection between the vee-splitter and the feed pipes consists of lengths of flexible tubing, installed to simplify the withdrawal operation.

The delivery system is driven by an exhaust system powered by a pump capable of delivering 500 scfm at a 15" vacuum, exhausting from the simulator vent via two fines separators and a cartridge type filter in series, and discharging to atmosphere through a long fiberglass pipe terminating outside the building. This exhaust system provided the stream of air at the velocity necessary to entrain the packing components, as described above.

A schematic layout of the system is presented in Figure 4.

The amounts of material processed at the hoppers, and the amount of deposited packing actually delivered, were measured by calibrated load cells which supported each leg of each hopper and which supported the frames into which the simulator was set (see Figure 5). The outputs of these load cells were recorded as a function of time on paper tape. Other instrumentation included manometers and gauges for reading critical pressures, tachometers and rotational speed controllers for reading and adjusting the speeds of the feed mechanisms, and analytical balances for measuring the masses needed for the calculation of densities and mineral concentrations of samples taken after each run. Figures 6 and 7 show the system instrumentation and control panels.

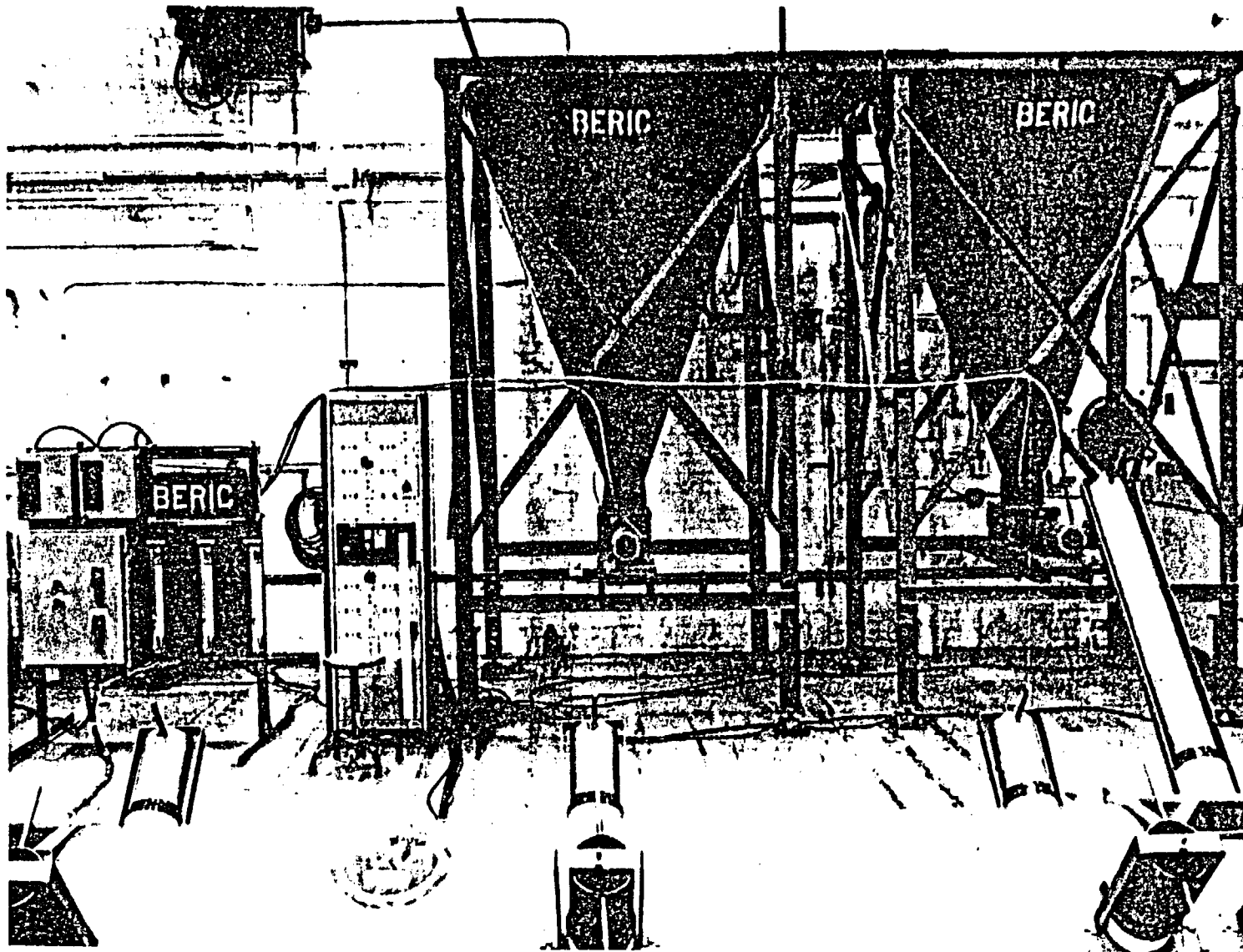
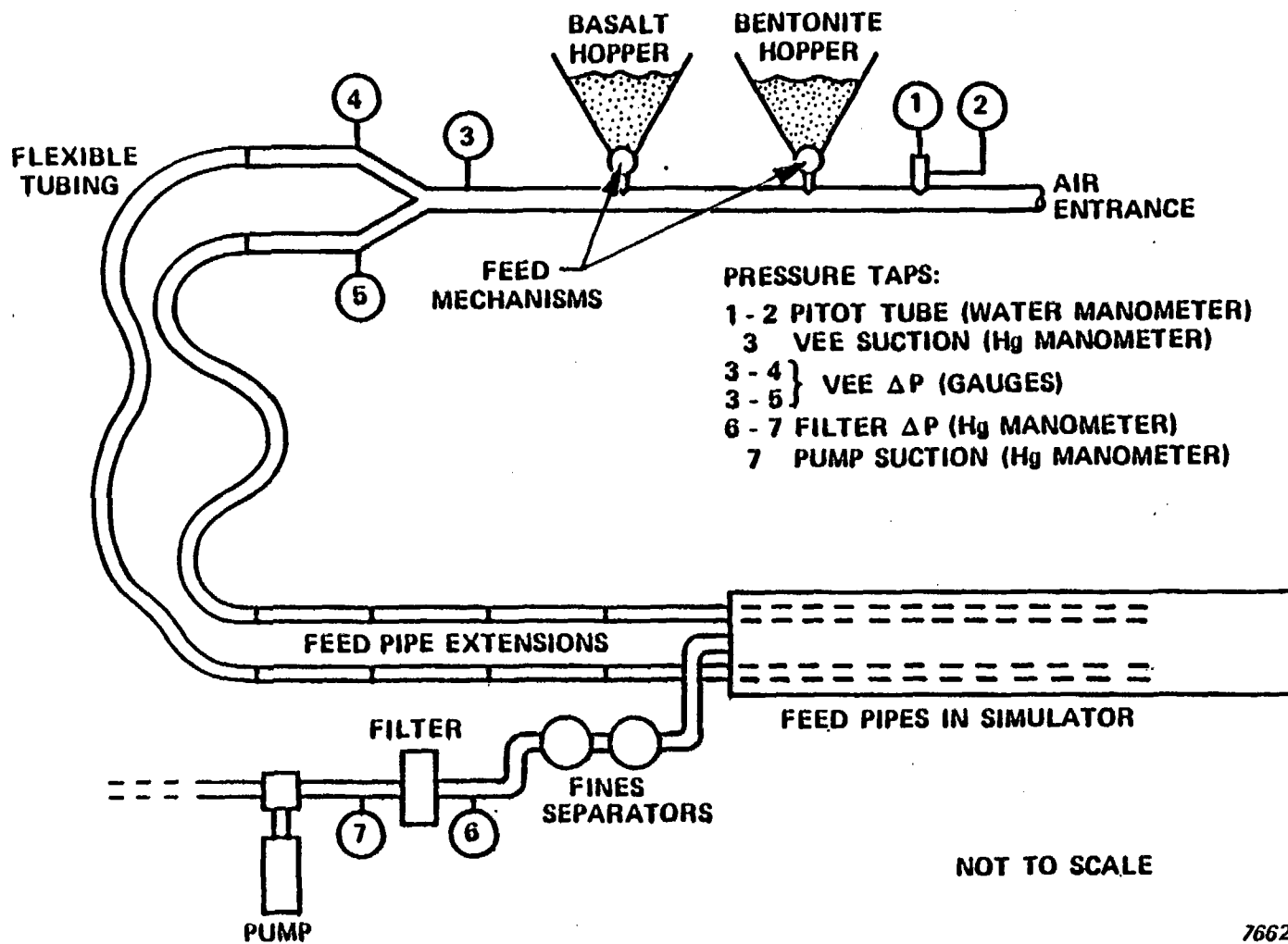


Figure 3. Feed Hoppers. Note feed motor mechanisms below each hopper and transfer tube running beneath hoppers and behind instrumentation at the left. The basalt hopper is to the left.

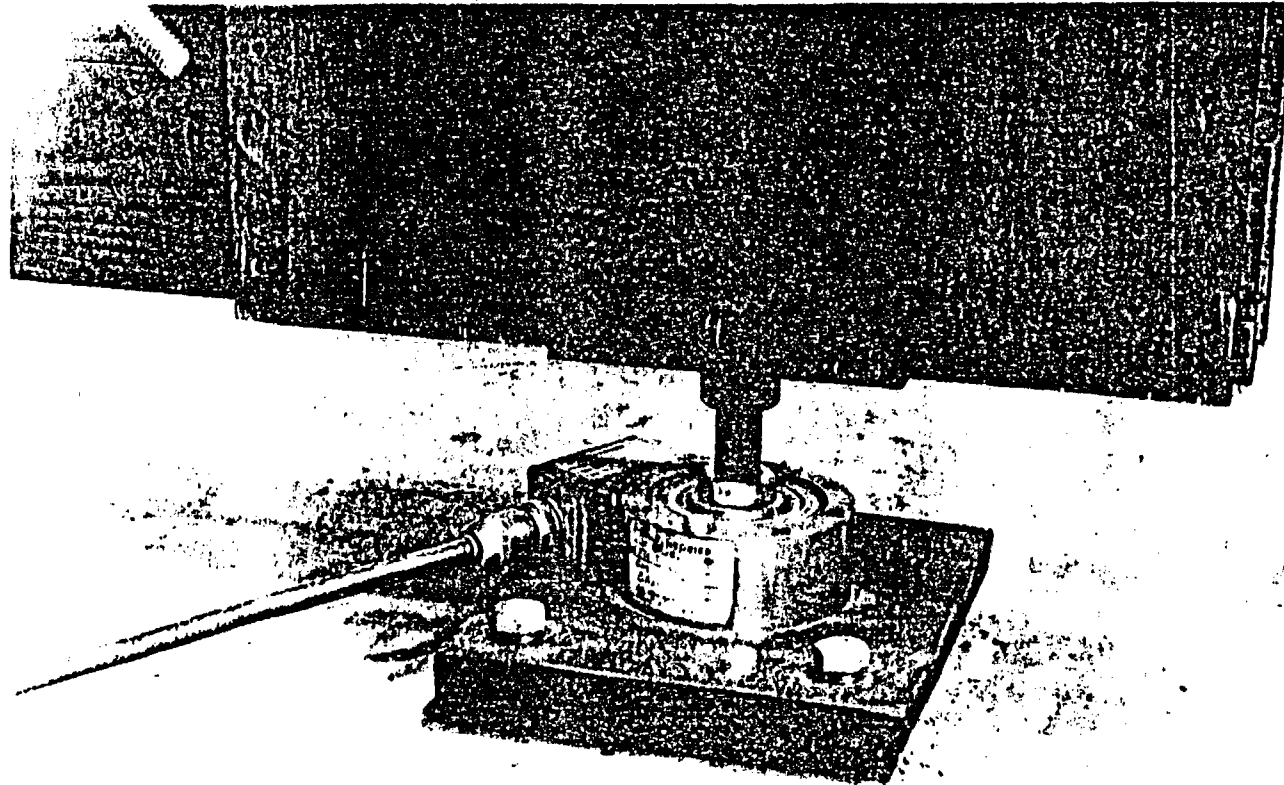
ITSD-TME-030
DRAFT



766270-2A

IITSD-THE-030
 DRAFT

Figure 4. Schematic Layout of Test System



9

HTSD-TME-030
DRAFT

Figure 5. Load Cell Showing How Hoppers and Simulators Are Supported

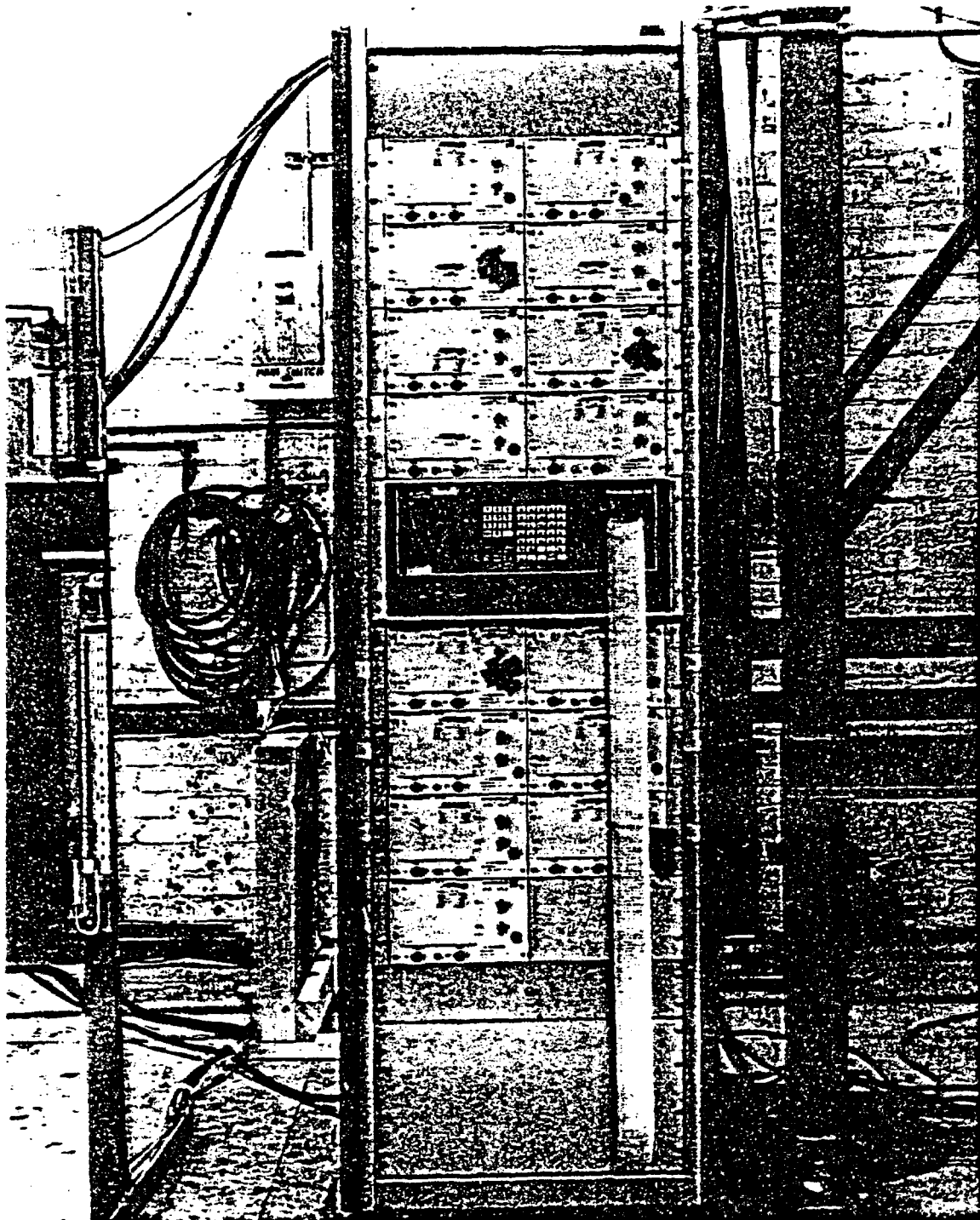


Figure 6. Load Cell Instrumentation Showing Amplifiers and Data Logger

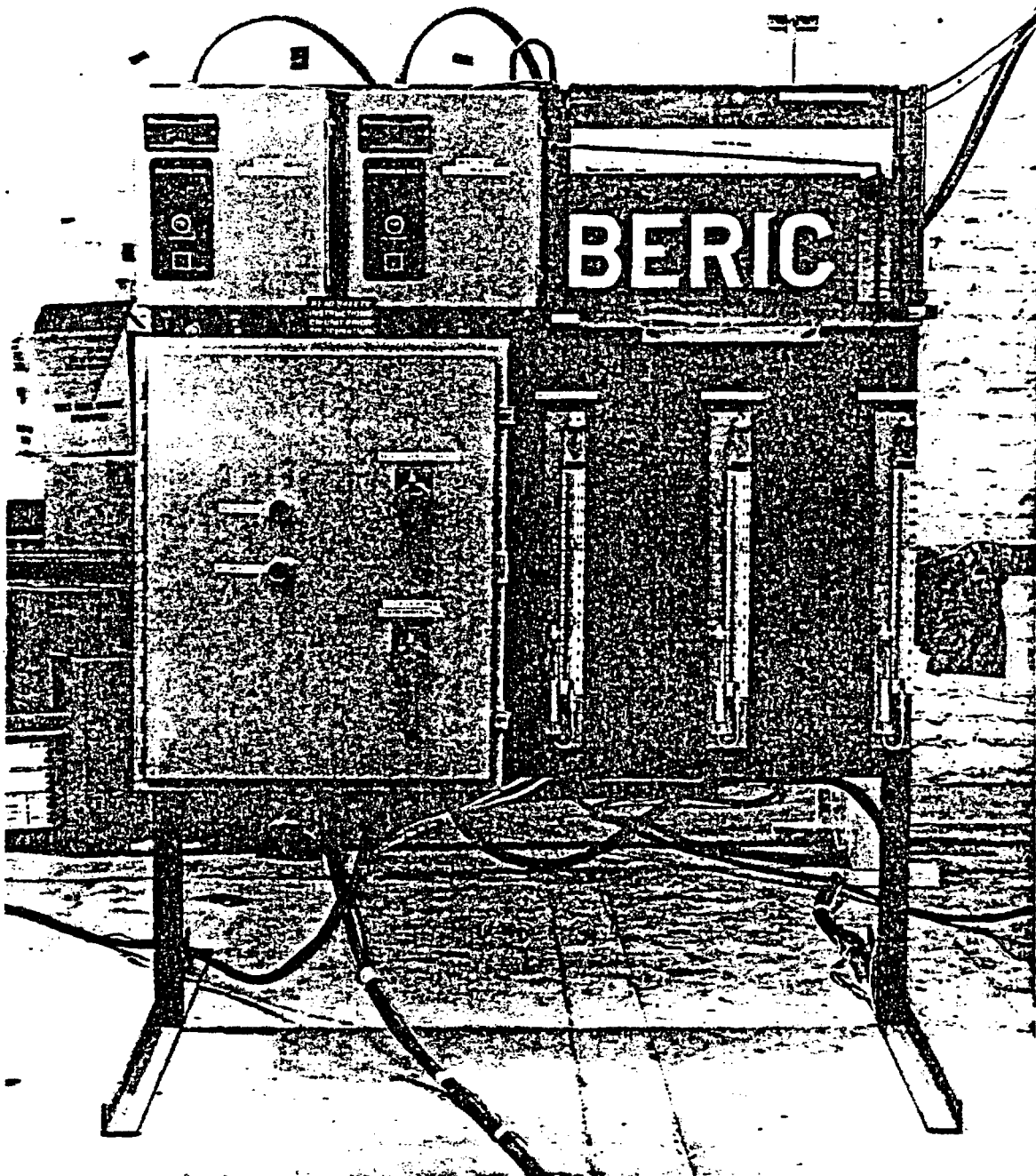


Figure 7. Pressure Instrumentation and Operations Control Panel

2.2 MATERIALS: BASALT AND BENTONITE

2.2.1 Characterization and Analysis

2.2.1.1 As-Received Materials

Both as-received materials were sampled; most of the samples were stored as library samples, and a number were devoted to various tests to characterize the incoming material, principally for moisture content and particle size distribution.

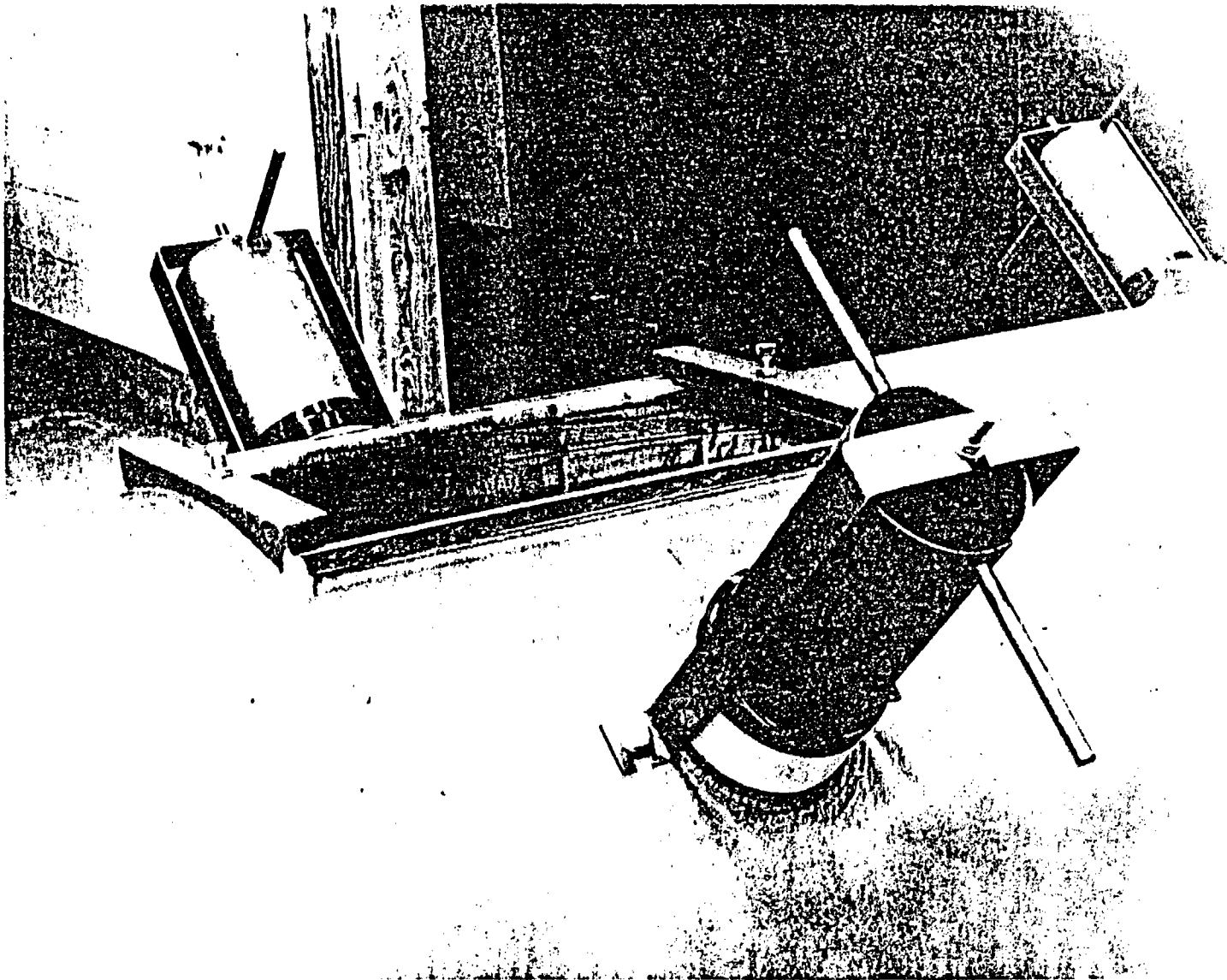
For particle size distribution, an array of standard sieves was used, the exact sieve numbers depending on the sieve grade standards as set out in the specifications for the two materials. About two hundred gram samples of material was placed in the uppermost sieve, and sieving was performed dry, using mechanical agitation. Sieve contents were weighed, and the distribution of weights was converted into the integral form as a table of "percent passing".

Percent moisture was determined for basalt by drying weighed as-received material for a few hours in a vacuum oven, and re-weighing when cool. Percent moisture was taken as the fractional weight loss x 100. Percent moisture was not determined for bentonite.

Tap densities were determined for the two materials and for a range of mixtures by placing the material in a weighed volumetric cylinder (graduate), and tapping firmly with a metal rod for several minutes until no further decrease in volume could be detected. The fractional density was taken as the measured density (weight/tap volume) divided by the theoretical density, which was taken as 2.7 g/cc for both materials.

2.2.3.2 Post Operations Analysis

At the conclusion of operations, after filling the simulator, the sampling cylinders, one of which is shown in Figure 8, were all driven inward until they seated, as described in Appendix A. The packing samples thus cored by the cylinders were then emptied into tared, labelled plastic containers with covers; the lower cylinders were emptied directly, by gravity, and the upper cylinders were emptied by using a small vacuum cleaner. The material in the various plastic containers was then analyzed for density and homogeneity as explained below.



13

Figure 8. Sample Cylinder. See Appendix A for a detailed description.

WTSD-TME-030
DRAFT

Densities were measured by weighing the contents of each sample cylinder in its prepared plastic container, and dividing the mass so obtained by the cylinder volume. The latter was determined from physical measurements, with a calculated correction for the scallop volume associated with the inner end of the cylinder (see Appendix A). The weighed material was then retained for use in the analytical determination of basalt concentration.

The measurement of basalt concentration is based on the removal of bentonite as a soil, leaving behind the insoluble basalt fraction. The procedure, as developed by Westinghouse during the course of this project, is presented in Appendix B. Several weighed portions of each well-mixed sample are treated successively with portions of water containing a water-softening agent, and shaken after each addition; after standing until the solids settle, excess liquid is siphoned off. The siphonate, after some six treatments, will have carried off essentially all the bentonite (as well as some basalt fines, for which a correction is introduced), leaving the basalt behind. The residue is filtered, dried and weighed. From the weight data, the percent basalt, percent bentonite, and the basalt to bentonite ratio can be calculated. The homogeneity of the emplaced basalt can be established, as explained in Appendix C, by a statistical comparison of the basalt concentration, established by the above procedure, at all sampling positions along the simulator.

2.2.2 Basalt

The basalt used in all four experiments was obtained directly from Rockwell Hanford Operation. This material was crushed basalt having an average particle size distribution as follows:

<u>Sieve Size</u>	<u>Percent Passing</u>	
	<u>Range</u>	<u>Average</u>
4.75mm (#4)	87 - 93	89
1.70 (#12)	32 - 53	39
1.18 (#16)	22 - 42	29
710 μ (#25)	12 - 29	18
500 (#35)	9 - 22	13
250 (#60)	5 - 13	7

1283I:25-13

The moisture content of this material was determined to be 2.86% with a standard deviation of 0.60%. The material dried quickly in air, and no experimental difficulties could later be assigned to the moisture level.

2.2.3 Bentonite

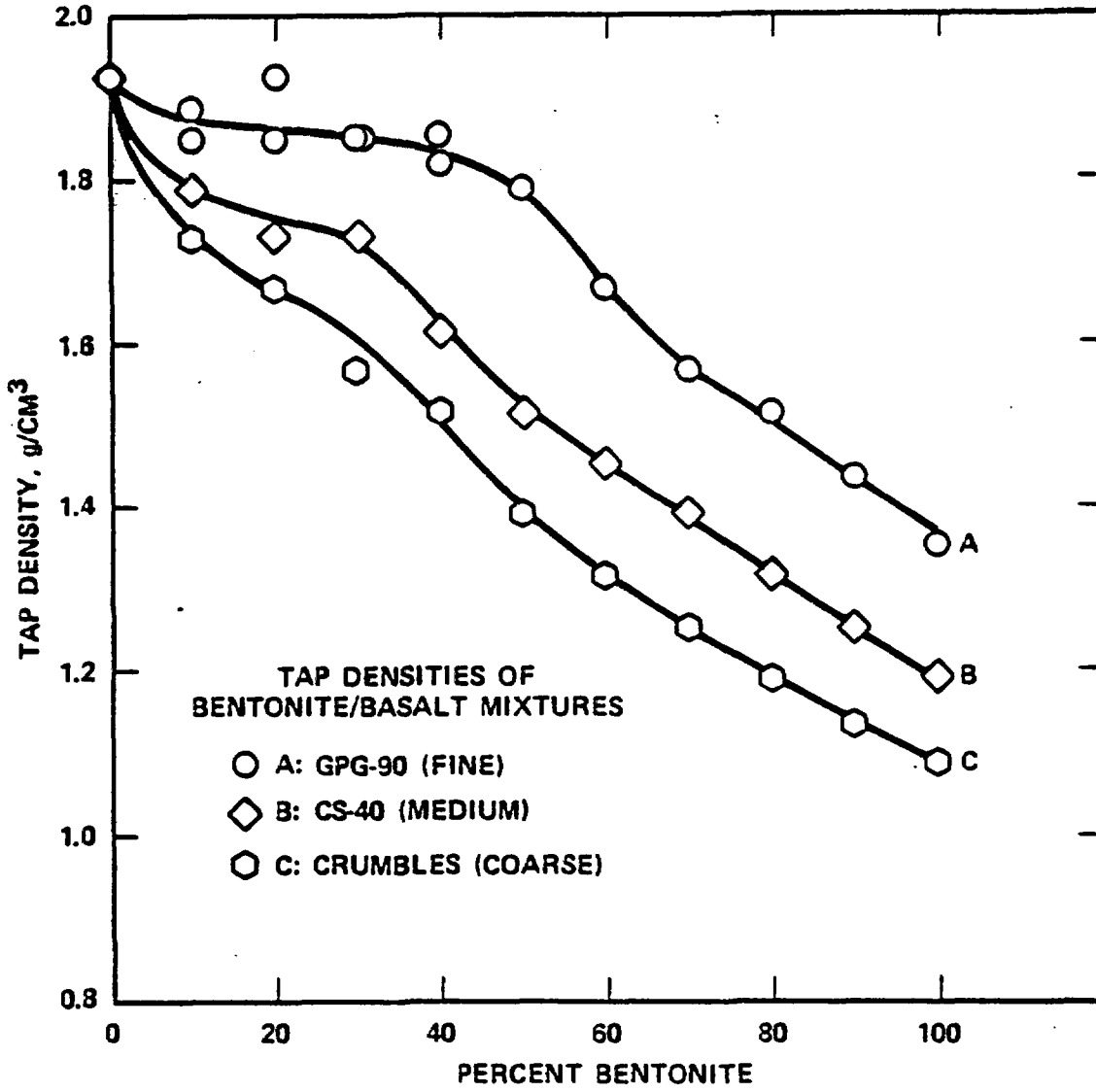
Bentonite was purchased from American Colloid according to the provisions of a specification which demanded natural, high swelling, sodium bentonite, free from foreign materials, adulterants, or additives. This specification provided sieve grading standards for coarse, fine, and broad range bentonite, as follows:

<u>Sieve Size</u>	<u>Percent Passing</u>		
	<u>Coarse</u>	<u>Fine</u>	<u>Broad Range</u>
3.35 mm (#6)	100	-	100
1.70 (#12)	60-80	-	-
850 μ m (#20)	10-30	-	60-80
600 (#30)	0-10	-	-
425 (#40)	-	100	-
212 (#70)	-	60-80	20-30
106 (#140)	-	10-30	-
75 (#200)	-	0-10	0-10

Other technical requirements included a maximum moisture content (10%), swelling (to pass test), calcium equivalent (0.70 percent max.), and wet screen analysis residue (4.0 wt.% max.). The vendor certified that all these requirements had been satisfied.

2.2.4 Packing

Tap densities were measured on a series of mixtures of basalt and bentonite mixtures across the range of composition, using all three grades of bentonite. The results are plotted in Figure 9 as tap density vs. percent bentonite, and the curves all show a monotonic decrease in tap density from 1.87 g/cc for undiluted basalt to less than 1.4 g/cc for undiluted bentonite. As one might expect, the curve for fine bentonite (GPG-90) lies higher than the one for coarse bentonite (Crumbles) by almost 0.3 g/cc over most of the range, with the curve for broad range material (CS-40) intermediate. This result suggests that the GPG-90 material would tend to produce the highest packing density of the three. All three curves exhibit a brief, almost horizontal, segment in the range 15 to 45 percent



766270-1

Figure 9. Tap Densities for Mixtures of Crushed Basalt with Each of Three Grades of Bentonite

bentonite, most pronounced for GPG-90, the fine grade material. This "bump" suggests that as bentonite is added to the mixture the bentonite must fill interstices between fragments of the coarser basalt, with little change in packing, before the initial decline in density can be resumed.

2.3 OPERATIONS

2.3.1 Preliminaries

Before beginning regular experimental operations, a number of preliminary activities were carried out. These are:

- (1) Development of an analytical procedure for determining the concentration of basalt in a basalt-bentonite mixture (Appendix B).
- (2) Performing characterization tests on as-received materials, including particle size distribution, moisture content, and tap density.
- (3) Assembly of equipment, including interconnection of all parts of the apparatus, hook-up of electrical power, and connection of all instrumentation. Assembly was carried out to a written procedure.
- (4) Loading of hoppers. This operation was performed by using a high-lift equipped with a high capacity carrier, pivoted on a horizontal axis; the carrier could be loaded with nearly half a ton of material at floor level, lifted, and its contents dumped into a hopper in a relatively easy operation.
- (5) Systematic testing of the system components, including pump operation, operation of the various gauges and manometers, operation of the feeder mechanisms beneath the hoppers, and the checking of all pipe and hose connections and mechanical closures.
- (6) Calibration of the feeder mechanisms (see Appendix A).

2.3.2 Conduct of Tests

A program for the conduct of testing operations, involving specific equipment layout, values of experimental parameters, and experimental procedures had been drawn up in advance of the first experiment with the help of the designers and suppliers of the pneumatic transport equipment (Beric Engineering), who, in effect, acted as consultants during the early stages of testing. Many of the assumptions and provisions of this test plan were sound and were continued throughout the course of testing; early experience, however, showed others unsuitable to the present purpose, and these had to be replaced or

abandoned. Because of such changes, the first two test series served largely for shakedown, hence it would be inappropriate to draw conclusions based on the data generated from them. For example, partial blockages occurred undetected on several occasions, leading to the deposit within the simulator of unmixed bentonite when there was a basalt blockage, and vice versa; thus the homogeneity could not be established. The first series actually consisted of seven separate runs, each with changed parameters and variations in configuration. These changes followed the following course:

- (1) Feeders blocked. Response: reseal all system leakage.
- (2) Vacuum improved but feeders still blocked, simulator not filled to top. Response: decrease feed rate, install upward pointed nozzles.
- (3) Blockage problem persists; blower discharge hose ruptures. Response: re-align vee splitter, alter blower discharge configuration and install fiberglass discharge tube.
- (4) Blockage problem persists. Response: increase frequency of feed pipe withdrawal.
- (5) Loss of flow velocity to below critical level because of filter clogging. Response: install fines collector in series ahead of filter.
- (6) Filter clogging and high pressure drop problem continued. Response: introduce second fines collector of improved design in series with first.
- (7) Simulator was filled, but filter problem remained unsolved.

The second series was aborted and the simulator emptied at an early stage because of a side-to-side maldistribution of deposited packing. Therefore, the data from these tests, with the exception of density data from the first test series, are regarded as non-representative.

Before discussing the final test procedures, the various steps taken to relieve shakedown problems and improve the test configuration and operation will be enumerated:

- (1) The vacuum tightness of the whole system was improved by installing better seals at all static joints and by using vacuum putty or mastic at joints frequently disturbed.
- (2) The original filter element, designed to trap particles 10 microns and smaller was replaced with one rated at 50 microns.
- (3) A fiberglass discharge line was installed to accept the pump discharge, replacing the original plastic tube.

- (4) The initial vee-splitter arrangement, which created persistent problems in causing clogging of one or another of the split feed lines, was solved by installing the vee-splitter in the first run of feed pipe, upstream of the right angle bend, instead of in its original location, just after the first right angle bend. Subsequently, any delivery bias between the feed pipes could be rectified by minute changes in the angle at which the vee-splitter was set.
- (5) The original externally attached deflector nozzles at the feed tube discharges were replaced by deflector wedges internal to the feed tubes. These performed satisfactorily (although more development is needed) and are a first step in improving the feed tube design.
- (6) The fine grade of bentonite, designated GPG-90, was substituted in the later tests for the originally used coarse grade, Crumbles. This change was supported by the tap density tests described in Section 2.2.4.
- (7) The most expedient and economical method for emptying the simulator tube after filling it with packing and removing the required samples was to have it vacuumed by a commercial contractor. This could be accomplished in less than a day without disturbing the simulator, the waste package mockups, or the load cells, except for the temporary removal of the simulator windows.

Preparation for a test series required installation of the feed pipes into the fully inserted position, and their connection to the flexible hose which in turn connected to the branches of the vee-splitter. The sampling devices were set in place in the fully withdrawn position and properly sealed to retain vacuum. The plastic windows were installed with sealant along all edges. Filter elements were cleaned, and a 50 micron element installed in the filter. The appropriate amounts of basalt and bentonite were introduced into the hoppers. The readings of all load cells were recorded and averaged, so that the pre-test weights of each hopper and of the simulator were known and on record. The target feed rates were set on the feed screw motor counters, using the prior calibration curves. Test purpose and all initial condition data were recorded on the test data first sheet, a sample copy of which appears in Appendix D. The data logger was set to record load cell readings at five minute intervals (during the various shutdowns, the readings would be suspended).

To start the run, the blower was started, after which the two feed screw motors were turned on simultaneously. The time of day, all manometer and gauge readings and the tachometer readings were recorded immediately, and subsequently at short (1 to 4 minute) intervals, throughout the run (downtimes excepted). These data and incidental comments describing test progress are recorded on follow data sheets, a sample of which also appears in Appendix D. More detailed comments were recorded orally with a mini-tape recorder.

As accumulation of packing begins, the profile of the deposit becomes visible at the one side window, located near the "back" end of the simulator. By timing the motion of the deposit profile, the fill rate of the simulator can be estimated, both at the side window, where the rearmost waste canister mockup occupies a portion of the simulator volume, and by cross-sectional area extrapolation, at inter-mockup spaces. For each test, the rate of pipe removal is fixed in terms of the fill rate so estimated and the schedule of the shutdowns for pipe withdrawal is thereby fixed early in the experimental process.

When the deposit profile has advanced to within a few inches of the initial position of the feed pipe nozzle, as established by calculation from the known fill rate, the feed screw motors and the blower are shut off in sequence. The nuts aligning the feed pipe exit glands are loosened, and a light steel cable is extended from a yoke clamped to the feed pipes to a winch some 30 meters away (see Figure 2). The winch is used to withdraw the feed pipes the desired distance from the simulator. The gland bolts are then retightened, and the vacuum putty seal, which is broken by the pipe movement, is remade. Pump and motors are restarted, and the run continues.

At several withdrawal shutdowns during the run, the feed pipe withdrawal brings the terminal feed pipe extensions close to the limit of flexibility of the flexible tubing portion of the transfer tubing. At this point the flexible tubing connections to these extensions are broken, and the two meter long extension pipes are removed. The flexible tubing ends are connected to the next extensions in line (or, late in the run, to the feed pipes themselves). The regular shutdown-startup procedure is then concluded, and the run is continued.

The feed pipes are withdrawn during the test until the nozzles are ultimately flush with the internal wall of the end plate. The simulator tube never completely fills; the exhaust connection, mounted high in the end plate (see Figure 2) withdraws material above this level, leaving a wedge shaped cavity in the simulator bounded by the cylinder walls, the upper part of the end plate, and the slope of the deposited packing surface profile. Prolonged operation after this configuration develops simply begins to fill the baffled fines collectors, next in the exhaust line. Accordingly, the run is terminated when the void volume appears to be constant. This void, whose volume is difficult to estimate, is a limiting factor in measuring the overall density of the emplaced packing as the quotient of delivered mass (from the load cell readings) and simulator volume.

2.3.3 Post-test Activities

After the final shutdown, final printouts of the load cell readings are obtained immediately, and the entire taped record removed from the logger and stored.

As soon as practicable, the sampling cylinders are inserted into the simulator tube to isolate the sample material. This is readily done with the 36 short cylinders and with the two of intermediate length. The five long, full diameter cylinders were found to be impossible to force in until they seated against the opposite wall; they had to be driven the last foot or so by sledge impacts through a protective thickness of lumber. The effect of such impacts on the packing material in and around these cylinders was necessarily severe enough to render their samples suspect for measuring either density or homogeneity, and the data from these samplers were largely ignored.

The samples are removed from the respective tubes into tared, labelled plastic containers, as described earlier, and weighed, to get density data. The material is then analyzed for basalt content, also as described earlier. When all samples have been removed, the cylinders are all withdrawn, and cleaned. Most of the windows are unsealed and removed, leaving the simulator sufficiently open so that vacuum removal of the packing can be done readily. The filter element is removed from the filter and cleaned. The filter and the two fines traps are emptied by vacuum at the same time as the simulator tube. After the simulator is empty, the feed pipes are replaced, and the extensions coupled on in series. The sampling cylinders are re-installed in the "out" position, and the windows replaced and sealed.

3 RESULTS AND DISCUSSION

3.1 OVERVIEW

The data of this project consists principally of the results of measurements from which densities and concentrations can be calculated. There are also experimental logs describing sequential activities and the chronology of various test parameters. Finally, there are the test observations as recorded in the test logs or on audio tape. The numerical results of measurements and the methodology for dealing with them are detailed in Appendix C, and summarized below. The system parameters under which operations were carried out are also summarized in this section. Finally, some general observations on test operations are enumerated and discussed.

3.2 DATA

3.2.1 System Parameters

Although optimum system parameters have not been developed, the parameters under which the system has operated successfully will be presented here. These parameters include hopper loadings, feed motor settings and tachometer readings, pressures, the rate of air flow, and the linear rate of fill of the simulator. In this context, the only values cited will be from the two final Runs, 3 and 4.

The simulator, with a free volume of 2.4 cubic meters (87 cubic feet), sustained a maximum fill weight of about 3900 kg (8600 lbs), corresponding to a total weight of about 6800 kg (15000 lbs). To provide this mass at a basalt:bentonite ratio of 3, the basalt was usually loaded to about 3400 kg (7500 lbs), giving a total hopper weight of about 4300 kg (9500 lbs), and the bentonite was loaded to about 1100 kg (2500 lbs), giving a hopper weight of 2000 kg (4500 lbs).

The feed motor speed controls were set to arbitrary scale readings of 179 for basalt and 112 for bentonite, corresponding to calibrated delivery rates of 0.237 and 0.079 kg/s, approximately one quarter of the rates that would fill the simulator to a density of 75% theoretical in one hour (see calibration curves, Figures 16 and 17, in Appendix A). During operation, these settings produced average tachometer readings which differed between the two runs:

Run #	Setting		Tach. Rdg. (rpm)	
	Basalt	Bentonite	Basalt	Bentonite
3	179	112	19.4	6.9
4	179	112	20.4	7.5

It is not clear why the average tachometer readings differed from each other and from the calibrated values, 18.5 and 7.1. The differences, which exceed the standard deviation, 0.3 rpm in all cases, do not appear to alter the as-filled component ratio, as will be seen below, but may be responsible for differences in total fill rate.

The suction pressure at the pump entrance is sensitive to the setting of the bleed valve, also located at the pump suction, the pump's internal relief valve setting (set to its maximum of 15 inches in all the present runs), and to the filter pressure drop. The latter depends on the filter load, which changes throughout the run, and the density of the filter cloth (we have used 10 micron and 50 micron cartridges). The filter pressure drop subtracts from the vacuum available in the system, and therefore affects the rate of air flow, as reflected in the Pitot tube manometer readings. Because of these variations, the pressure parameters below will be specified in ranges:

Vacuum at pump suction:	4.5 to 10.6 in of Hg
Vacuum at vee-splitter:	1.4 to 3.0 in of Hg
Filter pressure drop (50 micron)	0.2 to 0.4 in of Hg
Filter pressure drop (10 micron)	1.4 to 11.8 in of Hg
Pitot tube pressure difference	2.6 to 5.8 in of water
Simulator fill rate (at waste pkgs)	20 minutes per meter

The range of air velocities corresponding to the extremes of the Pitot tube pressure difference, according to the manufacturer's calibration, is 150 to 250 feet per second (50 to 75 meters per second), or, for the 2.5 inch schedule 40 transfer pipe being used here, 13,500 to 18000 SCFH (6.4 to 8.5 cubic meters per minute). Empirical calculations show that, as a rule of thumb, the solids velocity should be about 60% of the air velocity, ie, 90 to 150 feet per second (30 to 50 meters per second).

Tests 3 and 4 differed from each other in two significant respects:

- (1) For Run 2, the upward directing nozzles attached externally to the ends of the feed tubes had been removed and replaced by metal wedges spot welded inside the tube ends. The flat end of each wedge blocked about half of the exit area. For Run 3, the same wedges were used, so disposed that exit flow was upward directed from both feed pipes. For Run 4, the wedges were removed and split vertically somewhat off the horizontal center; the smaller pieces were exchanged, feed pipe to feed pipe, and inverted so that, when remounted in the feed tube ends, the feed flow would be diverted, somewhat more than half upwards, the rest downwards. This change was made for two reasons: (1) to try to densify the accumulating packing by direct impact of packing particles over the entire surface instead of just the upper part of the surface, and (2) to ensure that, although some of the material on the lower parts of the packing surface profile must originate by sliding down the profile slope after impacting on the upper part, this material will nevertheless be struck by particles of the freshly arriving, downward directed feed, be driven in, and thereby contribute to densification. The difference in nozzle design is shown in Figures 10 and 11.
- (2) For Test 3, the feed tubes were extracted in two-foot increments; for Test 4, they were withdrawn one foot each time the deposit profile advanced one foot. It was decided to withdraw only one foot at a time to keep the discharge nozzles at a more or less constant distance from the deposited packing profile. Obviously, this is impossible to do exactly without using continuous withdrawal, and even then, only if the location of the profile is always precisely known. Thus, withdrawal a foot at a time was a compromise.



HTSD-THE-030
DRAFT

Figure 10. Wedge Nozzles Directing Flow Upward, as Used in Run 3

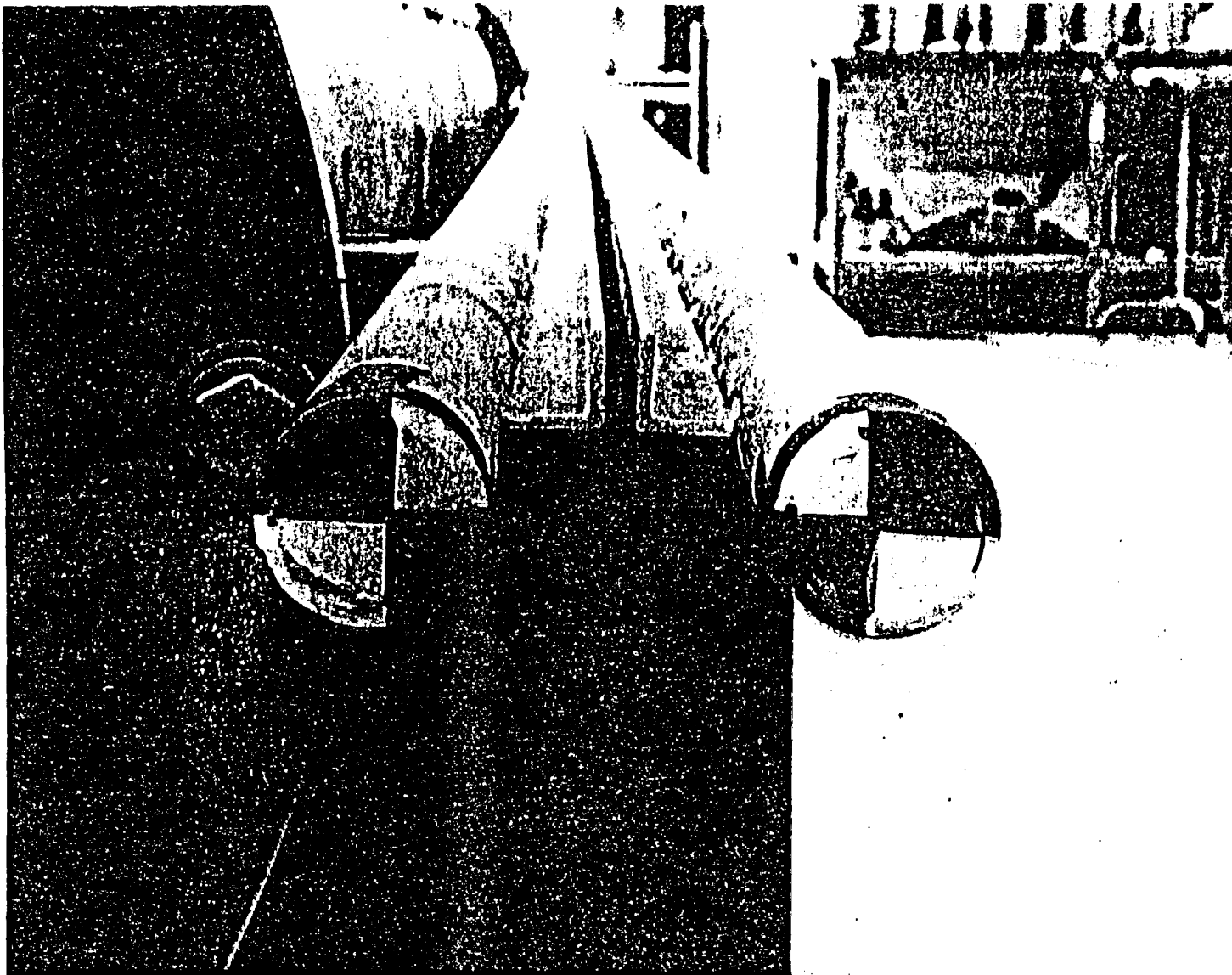


Figure 11. Wedge Nozzles Directing Flow Both Upward and Downward,
as Used in Run 4

MTSD-THE-030
DRAFT

3.2.2 Density

The results of all four test series are summarized below:

<u>Run #</u>	<u>Source</u>	<u>Density (g/cc)</u>			
		<u>Value</u>	<u>Std. dev.</u>	<u>95% Conf. Interval</u>	
1	Load cells	1.37	--	--	--
	Sampling	1.41	0.08	1.39	1.43
2	Load cells	--	--	--	--
	Sampling	1.59	0.09	--	--
3	Load cells	1.56	--	--	--
	Sampling	1.55	0.13	1.52	1.59
4	Load cells	1.59	--	--	--
	Sampling	1.56	0.10	1.54	1.59

The detailed density data and their statistical analysis are given in Appendix C.

As indicated earlier, the densities from the first two series, because of inconsistencies and irregularities in test operation, are not regarded as equivalent to the data from Series 3 and 4, to which the full analysis was applied. Nevertheless, the results of the latter, when compared to the results from the first test show a significant gain. On the other hand, compared with the desired 70% theoretical, the Series 3 and 4 results show a long way to go. In the figures above, the sample average is considered more reliable than the load cell average, because, although the load cell readings are highly precise, the presence of simulator voids, some observed and others possible, makes the true filled simulator volume uncertain. Of course a similar bias could exist in the volume of each sample cylinder, but since the number of samples is large (36), and the associated biases can be of either sign, averaging will tend to cancel out any effect.

As indicated in the above density results summary, a major increase in observed density accrued in Runs 2, 3 and 4 over Run 1. The only major experimental parameter that was changed in the same manner as the results varied was the bentonite size distribution. Thus, these density results are in agreement with the top density results presented in Figure 9 - a finer grade of bentonite results in a higher overall density.

The statistical studies in Appendix C show that while there is no significant difference in density in either test from side to side or from front to back of the simulator, in both tests there is a significant difference from top to bottom: the mean density in the top half is significantly greater than that in the bottom half. "Significant" is used here in the statistical sense: at the 95% confidence level, we believe that this result is not simply due to chance.

This result may arise from stronger direct impact of solid fragments of depositing material on the upper part of the packing profile because of the upward deflecting nozzle inserts. In Run 4 deflections were both upward and downward, but the accumulating mass in the lower part of the simulator, augmented by material sliding down the planted profile, tended to block the exit of the down-throwing wedge, choking any densifying action.

The general frequency distribution for density is presented in Figures 12 and 13. These figures show that while the bulk of the samples had densities in the range about the average, from 1.52 to 1.65 g/cc, the full range of the data extended from 1.32 to 1.82 g/cc. The latter figure is about 67% theoretical, and suggests that, since at least one region achieved that level, its attainment as an overall average is, at the very least, a practical possibility.

3.2.3 Mineral Homogeneity

The mean basalt concentration was close to the target value of 75% basalt in both tests; specifically, the grand average of all samples for Test 3 was 74.13%, and for Test 4 was 75.20%. The frequency distributions for the basalt concentrations in the two tests are given in Figures 14 and 15, where it can be seen that the overall homogeneity spread is reasonably narrow, especially in Test 4, and concentrated in a band between 70 and 80 percent. The detailed concentration data are given in Appendix C.

The statistical analysis of basalt concentration in Appendix C shows that in Run 4 there is a significantly higher basalt concentration in the upper quadrants of the simulator than in the lower. The difference is statistically significant, and cannot be reasonably explained as a result of random error. This difference is the only large scale inhomogeneity detected statistically in any of the six studies made (for each test, a contrast of top-to-bottom, side-to-side, and front-to-back). Unlike the case for density inhomogeneity discussed above, the concentration inhomogeneity is confined to one run.

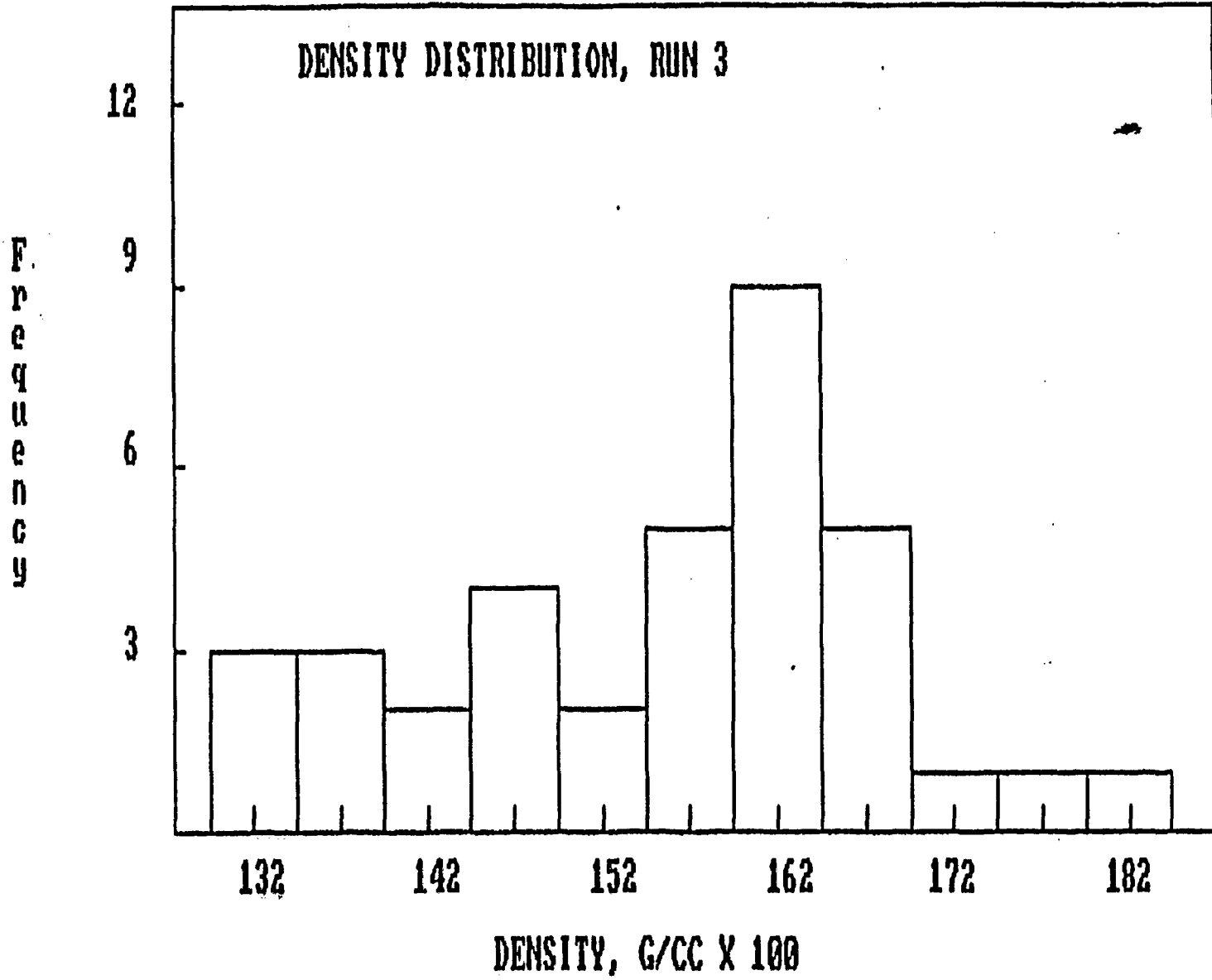


Figure 12. Density Distribution for Run 3

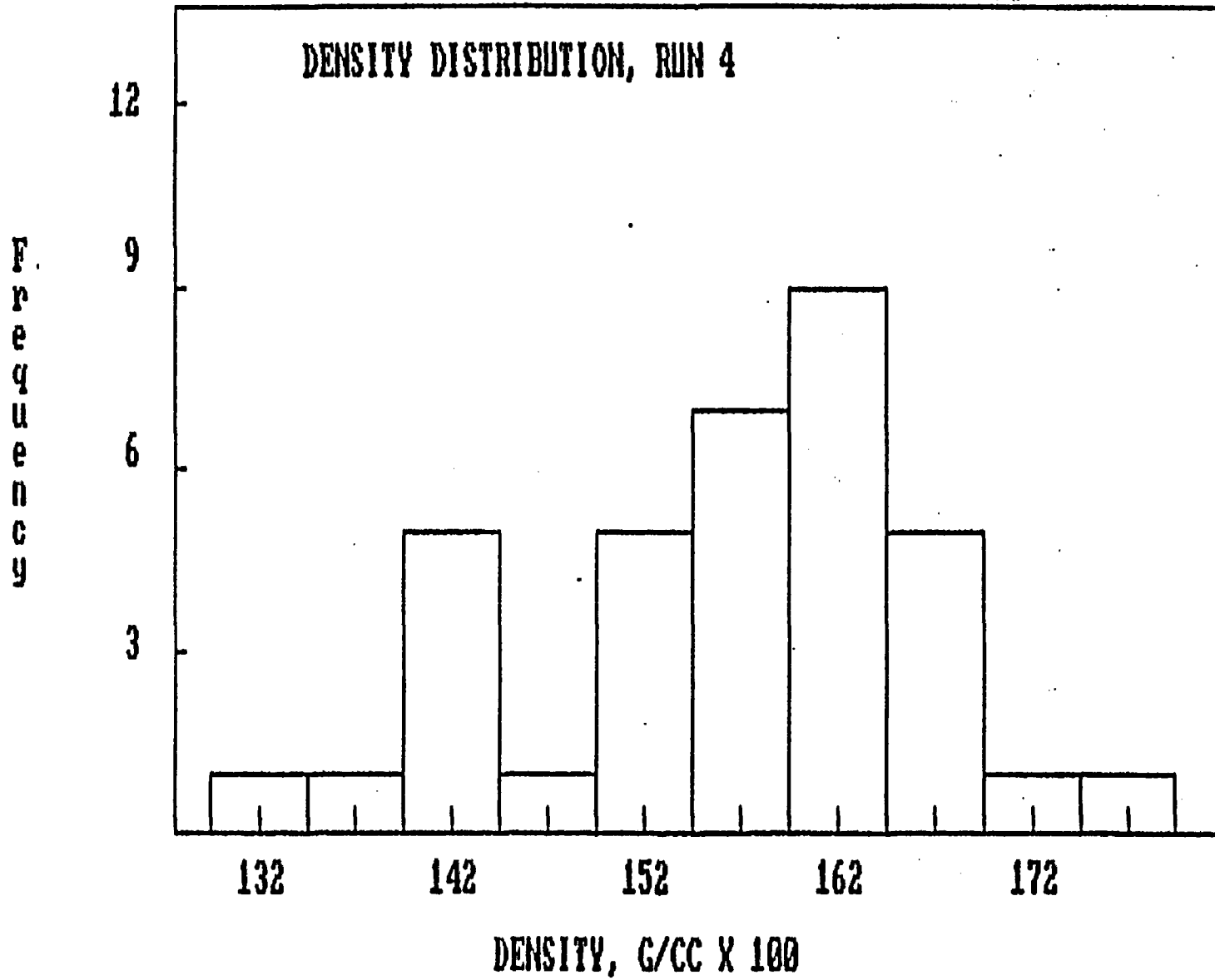


Figure 13. Density Distribution for Run 4

F
r
e
q
u
e
n
c
y

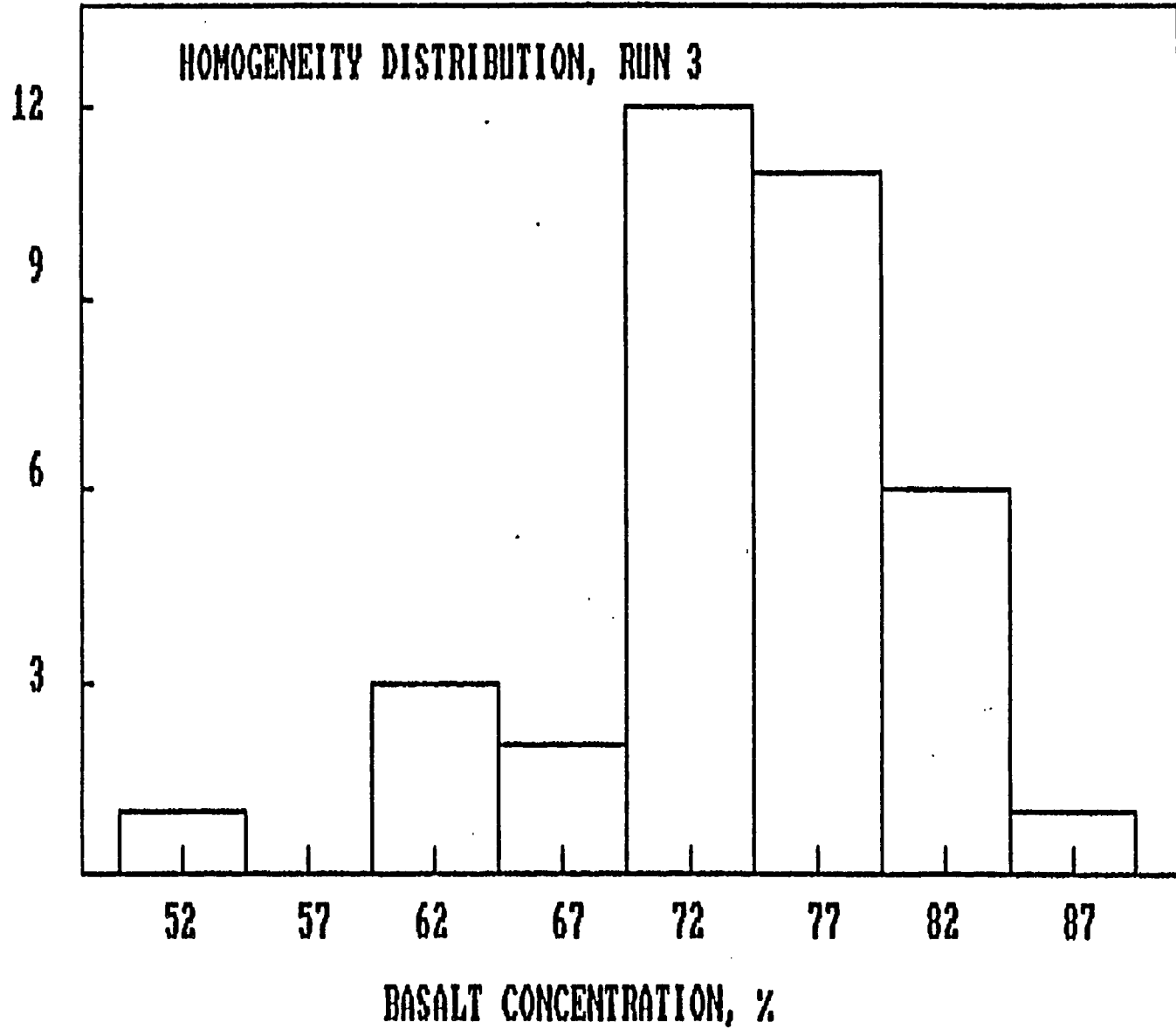


Figure 14. Basalt Concentration Distribution for Run 3

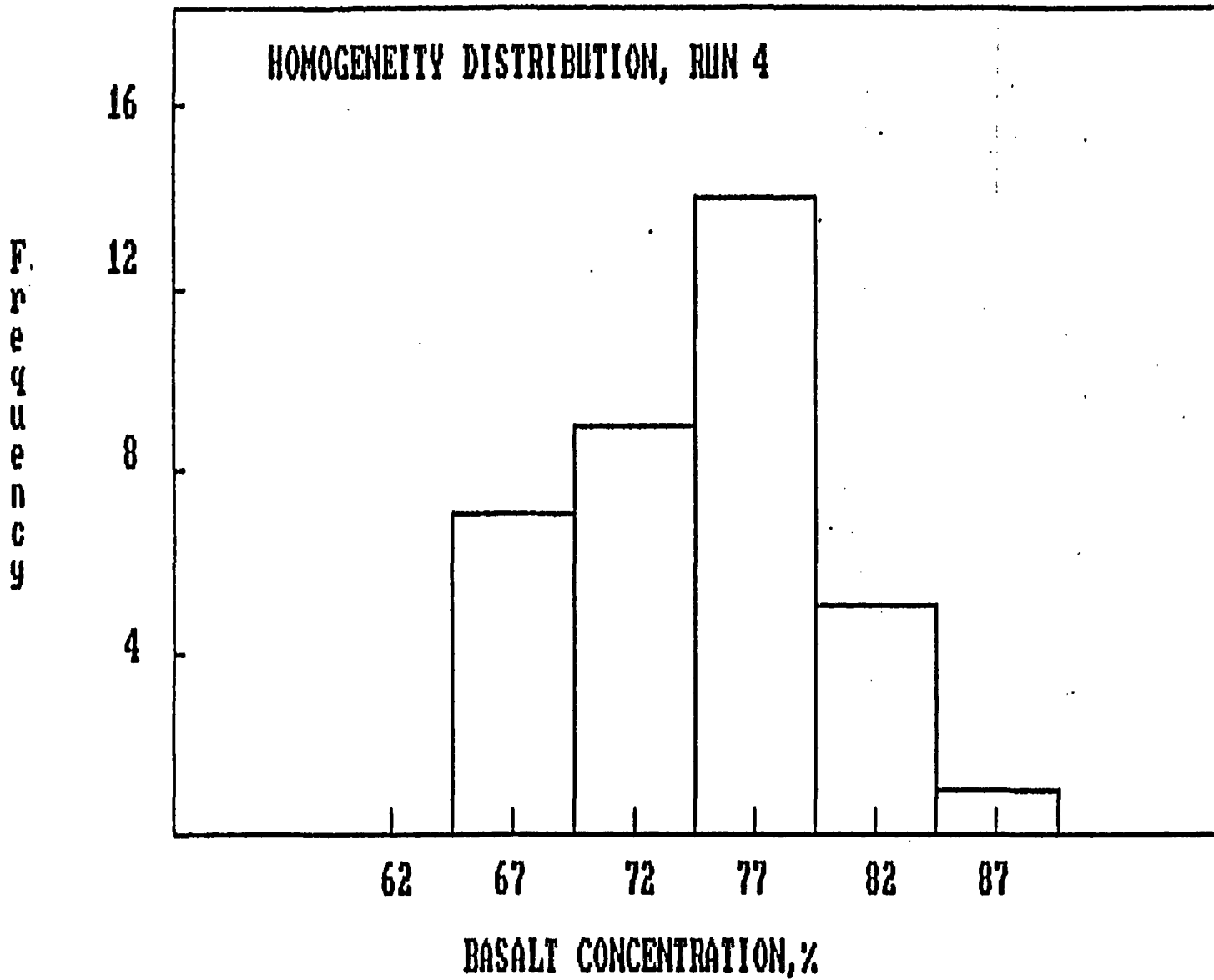


Figure 15. Basalt Concentration Distribution for Run 4

However, the statistical studies consistently, in all six runs, indicated that the dominant component of test variance is associated with the sampling, one sample being associated with each of the 36 short sampling cylinders. The significance of this finding is that there is a mid-scale graininess in the inhomogeneity developed by the emplacement configuration used: The averaging of the sample basalt concentration produces reasonably low variability when large, several ton, "batches" are contrasted, and the analysis of sub-samples, three of which were extracted from each sample, also produced a reasonably low variability; both are low in comparison with the sample-to-sample variability. Thus the emplaced packing is characterized by a kind of "clumped" inhomogeneity, and from the size of the sampling cylinders and their relative placement in the simulator tube, we can guess the "clump" size to be from a few liters to a few tens of liters.

3.2.4 Interactions

A large number of possible parameter interactions was investigated, both by plotting data and by computation of correlation coefficients, without finding any meaningful relationships. The various interactions looked at are discussed in Appendix C. Although some of the interactions considered produced suggestive correlations, it was concluded that no real correlations exist, and that the appearance of correlation, where it occurred, was accidental. Actually, the range of basalt concentration measured in these tests is too short to have an effect on packed density commensurate with the measured density range. Likewise, it is not clear how the deposited density could be a cause of, or generally correlate with, the local basalt concentration. It is probable that the two are independent, and responsive only to the feed ratio and to the local aerodynamic situation at deposition time, the parameters governing which are not accessible in the present experimental configuration.

3.3 GENERAL OBSERVATIONS

In general, this test configuration was successful in generating the data it was designed to: depositing a packing mineral mixture by pneumatic transport, and measuring its density and homogeneity. During the course of experimentation it was realized that the further task of optimizing the density to the desired level could not be achieved by the process of varying the accessible test parameters, as originally hoped, but would require alteration of procedures and some redesign of hardware. In this section various aspects of test design and operation will be evaluated in recognition of the present gap in the attainment of the desired density.

A number of parameters whose effect on emplaced density is uncertain, have not yet been varied systematically, so that the effects may be estimated. Among these are basalt size distribution, basalt to bentonite ratio, solids feed rate, solids water content, water content of transport air, air velocity, and nozzle throw distance. Optimizing this set of variables would be helpful, but would not guarantee reaching the target density.

The present need for a shutdown each time a feed tube withdrawal is made creates a discontinuity in operations which has adverse effects. Breaking and remaking the vacuum disturbs the already emplaced packing deposit, causing eddies as air moves first into and then out of the porous mass, entraining and redistributing particles of the solids. The net effect is to cause channeling and a general loosening of the deposited material, which can easily be seen at one of the windows, where the well-packed pre-shutdown deposit configuration changes completely, becoming multi-channeled and formless. This effect undoubtedly contributes to a low density, and is reiterated at each shutdown.

Finally, a number of observations are pertinent to the effect of the feed pipe wedge nozzles on the delivery of the packing. It was shown in the preceding sections that there were no significant gains either in an increased packing density or in simplicity of operations which can be ascribed to any of the changed features employed between Runs 3 and 4. It follows that the mechanism of direct impact all along the slope of the developing packing profile, which was indicated in an earlier section as a possible means of increasing densification, did not appear to work, although the impacts were indeed observed through the one side window available for this kind of observation. On the other hand, it was also observed that the down-throw feature employed in Run 4 was to a large extent self-defeating, because it led to a rapidly accumulating mass of material at a low level within the simulator. This mass, augmented by the material flowing down the slanted profile of the deposit, tended to block the exit of the down-throwing wedge, choking any densifying action, while the up-throwing wedge continued its normal pattern. This situation was probably abetted by the withdrawal schedule; withdrawal for longer distances at longer intervals might have prolonged the period before the down-throwing wedge was choked off.

4 CONCLUSIONS

1. In two successive tests, a 3:1 basalt and bentonite packing mixture was pneumatically emplaced in a borehole simulator tube at a density of 1.56 g/cc with reasonable mineral composition homogeneity.
2. A finer grade of bentonite resulted in a higher overall density as predicted by laboratory scale tests.
3. A statistical study of the density and homogeneity data from these tests has been carried out and reveals the following:
 - (a) In both tests the density of the upper layer of deposited packing was significantly greater than in the bottom layer.
 - (b) In the second of these tests (Test 4), the basalt concentration in the upper layer of deposited packing was significantly greater than in the bottom layer.
 - (c) Analysis of variance shows that the dominant source of variability within the overall packing material assay lies in the sampling process, suggesting that an irregular, "clumped", inhomogeneity exists in the emplaced material, the clumps having a volume from a few liters to a few tens of liters.
4. Values of system operating parameters have been developed, which, while not optimized, are adequate for successful operation of the packing equipment, and which can serve as an operating basis for future development and upgrading of system capabilities.

5 RECOMMENDATIONS

The following recommendations for increasing the packing density are appropriate.

5.1 WATER ADDITION

Based on the observation that the densities in the upper portion of the simulated borehole were higher than those in the lower portion and on the hypothesis that this density difference resulted from impact packing in the upper portion and from particle flow from the upper portion to the lower portion, a sticky packing should result in higher overall density. Since sticky particles should not flow, the upper portion density should be achieved over the entire simulated borehole using the upward-downward nozzle design from Run 4. Thus, an additional run using wet packing components or water addition in the feed stream is recommended.

5.2 FINER GRADE BENTONITE

As discussed previously the average density measured from Runs 2, 3, and 4 was much higher than in Run 1. Since the major difference between these runs was the use of a finer grade of bentonite, an even finer grade of bentonite could produce higher densities. Thus an additional run with a finer grade of bentonite is recommended.

5.3 SLOW VACUUM RELEASE

During the experimental runs, it was observed that when the blower was stopped and the vacuum in the test chamber broken the air movements in the chamber caused particle movements that probably reduced the measured density. Thus, the system should either be connected to a positive pressure system (which would result in expensive system modifications and safety problems) or a method of slowly reducing the vacuum incorporated. A run in which the vacuum is slowly created and eliminated is therefore recommended.

5.4 LOWER BASALT TO BENTONITE RATIO

In addition to the above recommendations, that should result in an increased packing density, another approach is possible to lowering the packing hydraulic conductivity (the objective of higher packing density). A lower hydraulic conductivity would result from additional bentonite in the same volume. Increasing the overall packing density is one approach. The second is to decrease the amount of basalt, therefore, leaving room for additional bentonite. Using a basalt to bentonite ratio of 2:1 or 1:1 should significantly lower packing hydraulic conductivity while still providing sufficient basalt for chemical buffering.

6 REFERENCES

1. Raymond Kaiser Engineers/Parsons, Brinckerhoff, Quade and Douglas, 1983. Conceptual Design Description, Nuclear Waste Repository in Basalt, Project 8-301, SD-BWI-SD-005 Vol. 1, Rockwell Hanford Operations, April.
2. Westinghouse Electric Company, 1982. Waste Package Concepts for Use in Conceptual Design of Nuclear Waste Repository in Basalt, RHO-8W-CR-136P/AESD-TME-3142, Rockwell Hanford Operations, April.
3. Leva, Max, 1959. Fluidization, McGraw-Hill, New York.
4. Box, G. E. P., W. G. Hunter, and J. S. Hunter, 1978. Statistics for Experimenters, John Wiley, New York.

7 APPENDIXES

APPENDIX A
APPARATUS

A.1 TEST SECTION

In the following sections, Westinghouse Drawing Identification Numbers are given in parentheses; the drawings are attached.

The borehole simulator is approximately 27 feet long, and contains three waste canister mockups, and the packing feed pipe supports. This configuration simulates the conceptual design for emplacement of Commercial High-Level Waste in the NWRB (References 1 and 2). The borehole simulator components consist of the main body and cover assemblies and equipment for support of the packing feed pipes, packing sampling, and viewing of the packing installation. The main body assembly is comprised of the main body, two flanges, 41 sampling ports, and seven viewing ports. The main body is a 30 inch outside diameter by 0.375 inch wall carbon steel pipe, 27 feet long. The material composition for the pipe is specified as AISI 1010/1030 for compatibility between the material of the pipe and those components to be welded to it, so that they could be joined by inexpensive, conventional welding. A standard 30 inch, slip-on carbon steel flange is welded to each end of the main body. This flange is a ring, approximately one inch thick, having an inside diameter slightly greater than 30 inches and an outside diameter of 38.75 inches. The inside diameter of the flange pilots over the ends of the pipe. The outside faces of the flanges are located 0.5 inch beyond the end of the pipe. They are secured with twelve short fillet welds between the end edge of pipe and the inside diameter of the flange plus another twelve short fillet welds on the outside of the pipe. The spaces between the welds were sealed by caulking. Each flange contains predrilled holes, 1.38 inches diameter, on a 36 inch diameter bolt circle.

The main body assembly contains 41 sampling ports. The sampling ports are 4.06 inch diameter holes formed by thirty-six (36) 3.00 inch long guide tubes (103E519It3) welded into the main body and five (5) 6.00 inch long guide tubes (103E519It9). These sampling ports are arranged in two functional groups as follows:

- o Thirty-six sampling ports are located to obtain packing samples from the annulus between the outside wall and the waste canister mockups. These are arranged in nine groups of four each. The individual ports are located at angles of 45, 135, 225, and 315 degrees from the vertical on the main body circumference. For each waste canister mockup, four ports are located approximately one foot from each end and the remaining four at the approximate waste canister mockup midlength.
- o Five sampling ports are located to obtain packing samples from the full diameter of the borehole simulator. There is one near each end of the main body assembly, outboard of the waste canister mockups, one between the front and middle waste canister mockups, and two, oriented 90 degrees apart, between the middle and rear waste canister mockups.
- o Two sampling ports are located on the back flange (opposite the feed and exhaust end), one above and to the right of the diametral center and one below it and to its left.

The viewing ports are 9 inch by 18 inch openings in the side of the main body pipe. There are seven viewing ports in the borehole simulator, located to provide visual access to areas of special interest and of differing cross section within it.

- o Two viewing ports are located at the "rear" of the simulator (the end away from the feed pipes and vacuum vent, the end which fills first), centered over the end of the rear waste canister mockup; one of these is on one side, 90 degrees from the other.
- o Three viewing ports are located along the length of the simulator, with one centered over the approximate middle of the rear waste canister mockup, one centered over the space between the rear and center waste canister mockups, and one centered over the space between the center and front waste canister mockups.
- o Two viewing ports are located on the "front" of the simulator. One is approximately centered over the end of the front waste canister mockup; the other covers the last 18-24 inches of the main body pipe. This will be the last portion of the mockup to be packed.

Six viewing ports are colinear; the seventh is located at the rear of the mockup, 90 degrees from the other rear viewing port. In all locations, the 9 inch dimension is an arc-length measured on the outside of the pipe; the 18 inch dimension of each cutout is in the direction of the pipe centerline. A 10 inch length of angle with a threaded hole (103E519 It4) is welded across each end of each view port. This feature is used to retain the view port cover. The viewing ports are covered with 0.50 inch thick clear polycarbonate windows approximately 17.5 inches long by 10.15 inches wide.

1283I:25-33

The end covers are 0.50 inch thick by 38.75 inch diameter carbon steel plates. The locations of only four of the predrilled holes in the flange were transferred to the end covers for use in bolting the covers to the flanges. A flange gasket (103E519 H17) is used with each cover. The rear end cover is comprised of the rear end cover plate (103E519 It6) and two sampling port guide tubes (103E519 It3). When the rear cover is assembled to the main body, the axes of these sampling ports are parallel to the main body axis, and within the projected envelope of the waste canister mockups. The front end cover plate (103E519 It7) contains two large holes for the passage of the packing feed pipes, two sets of four threaded holes for attachment of the packing feed pipe guides, three threaded holes for attachment of a dummy cover plate (103E519 H05), and a hole in which a 4.00 inch pipe half-coupling (103E519 It16) is placed, and welded to complete the assembly. A packing feed pipe gland assembly is mounted at each of the two large cover plate holes. Each consists of a length of 2.00 inch, schedule 40 pipe (103E519 It8), a pair of support angles (103E519 It9 and It10), a bearing plate (103E519 It11) and a mounting plate (103E519 It12). The mounting plate is cut out to allow passage of the packing feed pipe and its guide angle. A feedpipe gasket (103E519 H13) is used with each guide assembly. Each support is clamped in place using two angles (103E519 H14) and four bolts.

The packing sampling apparatus consists of sampling cylinders (103E518 G04, G05, and G06), piston inserts (103E518 G07, G08, and G09) and support brackets (103E518 H07, H08, and H09). All sampling cylinders are made of 4 inch O.D., 3.75 inch I.D. carbon steel tubing. There are three different sampling cylinder designs:

- o Thirty six (36) of the sampling cylinders (103E518 G04) are approximately 10.5 inches long with a fully-chamfered 9 inch radius "scallop" at one end. This 9 inch radius matches the curvature of the outside surface of the waste canister mockups.
- o Five (5) of the sampling cylinders (103E518 G05) are approximately 37.00 inches long and have a fully-chamfered 15 inch radius convex curvature at one end. These sampling cylinders are for the full diametral sampling ports where the stopping feature is the far inside surface of the borehole mockup pipe.
- o Two (2) of the sampling cylinders (103E518 G06) are 14.00 inches long and have a straight chamfered end. These sampling cylinders are for the rear cover of the borehole simulator where the insertion will be stopped by the flat plate head of the rear waste canister mockup.

Each sampling cylinder has an orientation line scribed into its outside surface. This line, matched to a scribe mark on the borehole simulator surface, is used to control the insertion of the cylinder, to ensure that its end configuration will properly match up to its stopping surface. The short, radial sample cylinders (103E518 G04) are stopped by the cylindrical surface of the waste canister mockups. The long, diametral cylinders (103E518 G05) are stopped by the far inside surface of the borehole pipe. The axial cylinders (103E518 G06) are stopped by the waste canister mockup flat head. Each type of sampling cylinder has an end configuration which matches that of the solid surface it will hit. This design detail aids in establishing a known-volume sample. Each sampling cylinder has two handles (103E519 It13), 4.50 inches long, made from 0.38 inch diameter carbon steel rod to aid insertion. The piston inserts are also identical, except for the length of the connecting rod. They consist of a disk (103E518 It14) machined to hold an "O" ring (103E518 It18) and welded to a connecting rod (103E518 It15, It16, or It17). The support brackets are identical except for length and the configuration at the inner end. The bolting holes are slotted to facilitate installation and removal.

The sampling cylinders are installed in their respective sampling ports together with the piston inserts and support brackets. The inner ends of the cylinders and pistons are then essentially flush with the inside surface of the borehole mockup. The cylinders are held in place by a set-screw in the sampling port guide tube while the support bracket retains the piston insert with two nuts at the piston insert outer end. The support bracket is secured to the emplacement mockup by two bolts. Electricians tape is used to seal the crevice between the cylinder and guide tube. The piston, inside the sampling cylinder, blocks its opening during packing and eliminates spillage as the sampling cylinder is pushed into the emplaced packing. The "O" ring, installed on the outside perimeter of the disc, provides reasonable surface-to-surface contact and seals the assembly against atmosphere.

The emplacement mockup contains three waste canister mockups which consist of a pipe body with flat plate heads. Support hardware for the packing feed pipes is attached to two of the waste canister mockups. The body of each waste canister mockup is an 18 inch outside diameter by 0.25 inch wall carbon steel pipe, 7 feet long (103E518 It1). The ends of the waste canister mockup are flat heads. Each head is 0.38 inch thick carbon steel plate with an outside diameter sized for a 0.030 inch diametral clearance to the inside diameter of the as-received pipe. Each head is partially inserted into the canister body and secured

to it with a 0.12 inch intermittent fillet weld (approximately 6 two inch long welds, equally-spaced on the circumference). This configuration adequately seals each waste canister mockup against filling during packing testing. One head of each waste canister mockup has a simulated handling pintle (103E518 It22). This simulated pintle (a 1.5 inch diameter bolt, 3 inches long) is included as a representative packing obstacle present in the NWRB conceptual design. It also serves as a test article handling device. Each waste canister mockup sits on four legs constructed of 6 inch by 2 inch structural tubing about 5.5 inches long. The legs, welded to the underside of the waste canister mockup pipe body, are 12 inches from each end of the waste canister mockup and are oriented in pairs at 45 degrees to each side of the vertical midplane. They center the waste canister mockup within the borehole mockup pipe and provide support for the packing feed pipe support brackets.

The packing feed pipe support brackets (103E518 G02) maintain the alignment, position, and orientation of the packing feed pipes while not constraining their withdrawal from the borehole mockup. Only the front and rear simulated waste canister mockups have the support brackets. This simplifies alignment requirements between brackets while still providing approximately equally-spaced supports for the packing feed pipes. The support brackets are fabricated from carbon steel plate. One bracket bolts to each of the four legs of the waste canister mockups. The upper part of the bracket forms a loosely-toleranced keyway for the structural angle which is welded to the packing feed pipe. A bolt (103E518 It24) and a pin (103E518 It6) provide radial and tangential restraint for the feed pipe assembly.

The emplacement hole mockup is supported on three wooden pedestals. Load cells placed under each pedestal are used to determine the weight of the installed packing material during testing.

A.2 FEED SYSTEM

The pneumatic conveying equipment was designed and built by Beric Engineering of Pittsburgh, Pa. It is a vacuum, dilute-phase system, capable of carrying, for a horizontal distance of at least 200 feet, a basalt-bentonite packing mix of arbitrary proportions at a rate on the order of 5 to 10 tons per hour. The feed section of this system consists of the following components:

1283I:25-36

- o Packing materials hoppers
- o Packing transfer tubes

A separate gravity-feed hopper is provided for each packing material. No premixing of the materials is required. Each hopper has a capacity of approximately 3.5 tons and delivers material to its own rotating screw conveyor. Each conveyor has a one horsepower, variable speed drive, which controls the relative quantities of material conveyed to the borehole simulator. The relative speeds of the two drives are fixed via a prior calibration to establish the desired 3:1 mixture ratio. A digital tachometer is included on each screw conveyor as a feed rate indicator. The outlet end of each screw conveyor is connected to an inlet of the infeed inducer. This chamber forms a transition between the screw conveyors on each side, atmospheric inlet air upstream, and the packing transfer tube downstream. Just downstream of the air inlet a Pitot tube connected to a slant manometer serves as an air flow meter. Each packing material hopper is supported on a base equipped with load cells. These load cells provide an on-line measure of input material weight.

The transfer tube line consists of 3 major sections of conveying pipeline arranged in a large "U" configuration, about 150 feet long. These sections are the fixed conveyor pipeline, a flexible hose section, and the packing feed pipes. The conveyor pipeline is made of multiple lengths of 2.5 inch diameter carbon steel pipe. This pipe run extends from the packing hoppers to a vee-splitter, where the flow is diverted to serve both borehole simulator feed pipes; at this point the transfer line diameter changes to 1.5 inches.

Each outlet of the vee-splitter is connected to a 30 foot length of 1.5 inch diameter flexible hose. The flexible sections allow the withdrawal of the packing feed pipes from the emplacement hole mockup, and are typical of sandblasting hose. They form a gradual 90 degree return elbow in the packing material pipeline. Each of the flexible hoses is connected to one of the packing feed pipes. These 1.5 inch diameter pipes are approximately 80 feet long. The last 25 feet of each feed pipe is initially inside the emplacement hole mockup. One pipe is positioned on each side of the waste canister mockups. The outer ends of these pipes are sections approximately 8 feet long. These sections can be disconnected and removed as the feed pipes are withdrawn from the emplacement hole mockup.

The inner ends of the packing feed pipes initially terminated in removable deflector nozzles to provide directional control for emplacing the packing in the mockup. Later, non-removable nozzles, integral with the tube ends, were designed and installed.

This feed section is supported on wooden pedestals, located at discrete points along its 200 foot length. The flexible hose section is supported at the same elevation as the metal transfer tubes.

A.3 EXHAUST SYSTEM

The vacuum pump and filter system are connected in series with one another and with the pipe coupling in the front cover of the borehole simulator. The three components are connected by two 10 foot long sections of 3 inch flexible hose. After some experience with the operation of the system, a pair of baffled fines traps constructed from steel drums was interposed between the borehole simulator and the filter.

A 20 horsepower 3-lobe rotary positive vacuum blower, manufactured by the M and D Pneumatics Co. of Springfield, MO, provides the primary motive force to convey the packing materials from the packing material hoppers through the transfer and feed tube system and into the emplacement hole mockup. The in-line filter system is included for the collection of dust in the effluent air from the emplacement hole mockup. The base of this freestanding filter system is supported on a platform balance to provide an on-line measure of trapped material weight.

A.4 INSTRUMENTATION

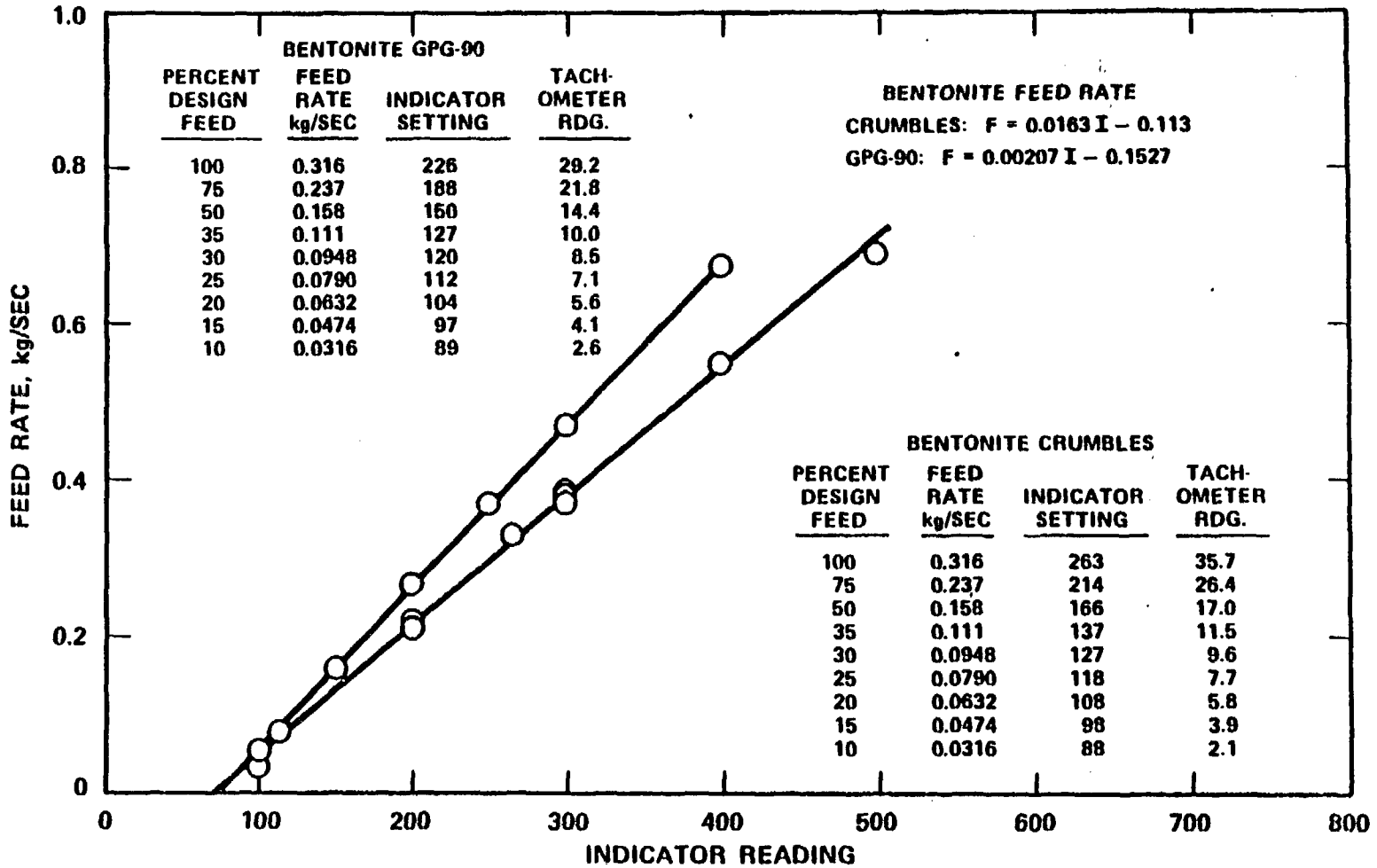
A total of 14 load cells is used to indicate equipment weight during packing operations; six of these load cells are used to support the borehole simulator and four are used to support each material feed hopper. The load cells are manufactured by BLH Electronics, Inc. located in Waltham, Mass. The output of the load cells is routed via individual calibrated signal conditioners, to a data logger, which can be set to scan all input signals and print out the results at arbitrary intervals. The printed tapes from all tests have been preserved

and constitute a record of all weight changes: processed weights for the hoppers, and delivered, or retained, weights for the borehole simulator. The processed weights and delivered weights differ by the amount of the losses experienced from various causes: fines passing through, losses incident to clearing lines from blockages, etc. Delivered weights are of course corrected for the weight of feed pipe removed from the simulator as filling proceeds.

Pressures indicated during packing operations by four manometers and two Bourdon type gauges, all mounted on a centrally located control panel. One manometer, an oil filled type, reads the differential between the static and pressure taps of the Pitot tube which is mounted in the transfer line upstream of the hoppers. The other manometers are all mercury filled; one reads the pressure across the filter element, another reads the differential between local atmosphere and the vacuum at the pump suction, and the third reads the same differential at the vee-splitter. Since in terms of pressure, manometers are absolute instruments, none required calibration. However, the Pitot tube manometer was calibrated in terms of air velocity by the manufacturer. The two gauges indicated the pressure differentials between the base of the vee-splitter and either arm; these indications are useful for detecting blockages in the arms, and calibration was unnecessary. Readings of all six of these pressure measuring instruments were recorded at frequent intervals during operations.

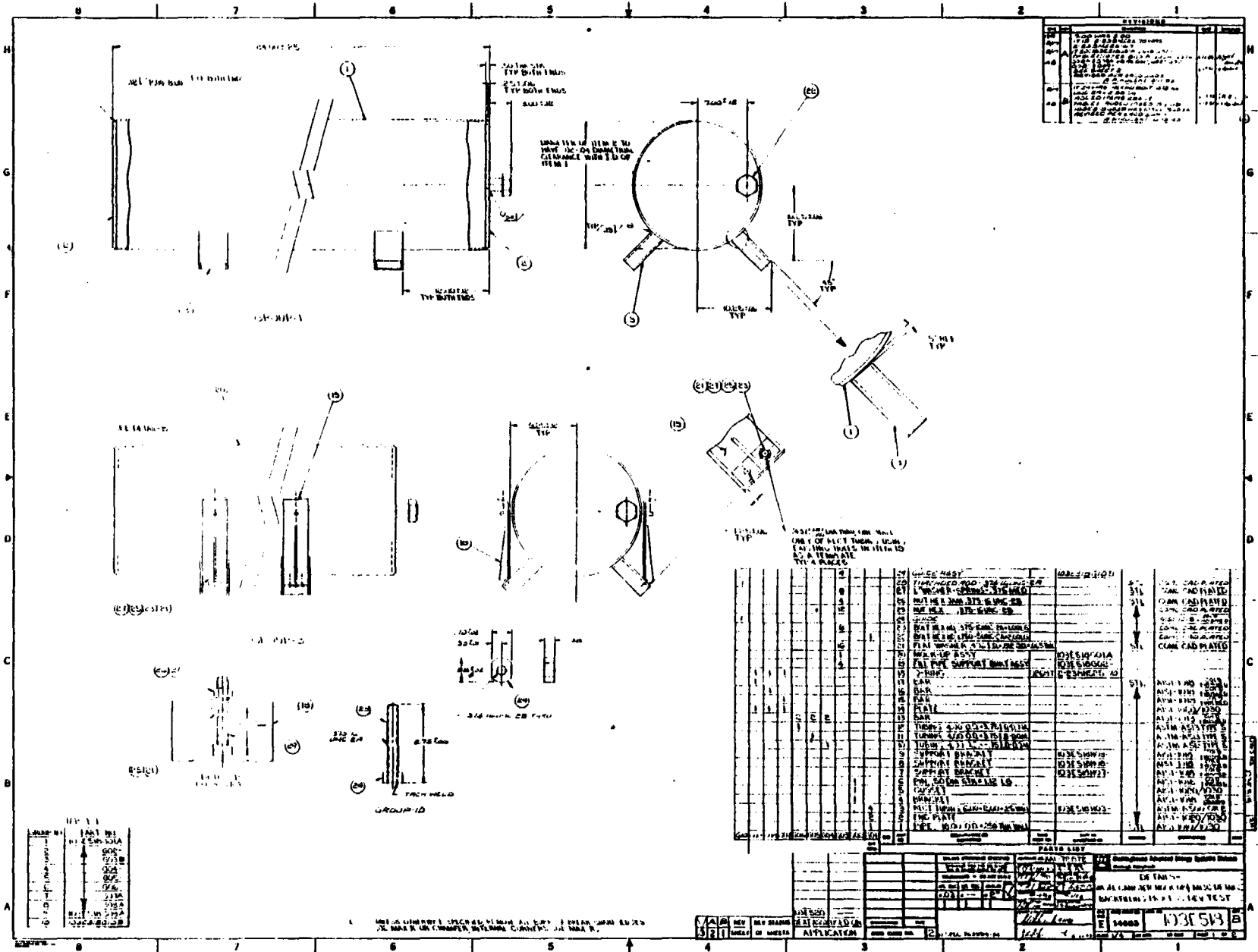
Feed rates were adjusted by controlling the rotational speed of the two feed screw motors, one at the discharge of each hopper. These speeds are adjusted by 1000 digit rotary counters mounted on the control panel, and the rotational speed read on the Nixie tubes of electronic tachometers, also mounted on the panel. The counter and tachometer readings were calibrated against feed rate by measuring the weight delivered into a tared receptacle for a measured time period, the transfer pipe being removed during the calibration operation. Calibration curves for the feed rates vs counter setting and vs tachometer setting are presented in Figures. 16 and 17.

The only other instruments in routine use were analytical balances, used for density and homogeneity measurements and for materials characterization measurements, as explained elsewhere. A calibrated platform balance was used for the feed screw calibrations (see above) and occasionally to measure the accumulation of fines in the filter.



766270-4

Figure 16. Calibration Curve for the Bentonite Hopper Feed Screw Mechanism, Feed Rate in kg/s Versus Feed Screw Controller Setting in Arbitrary Units



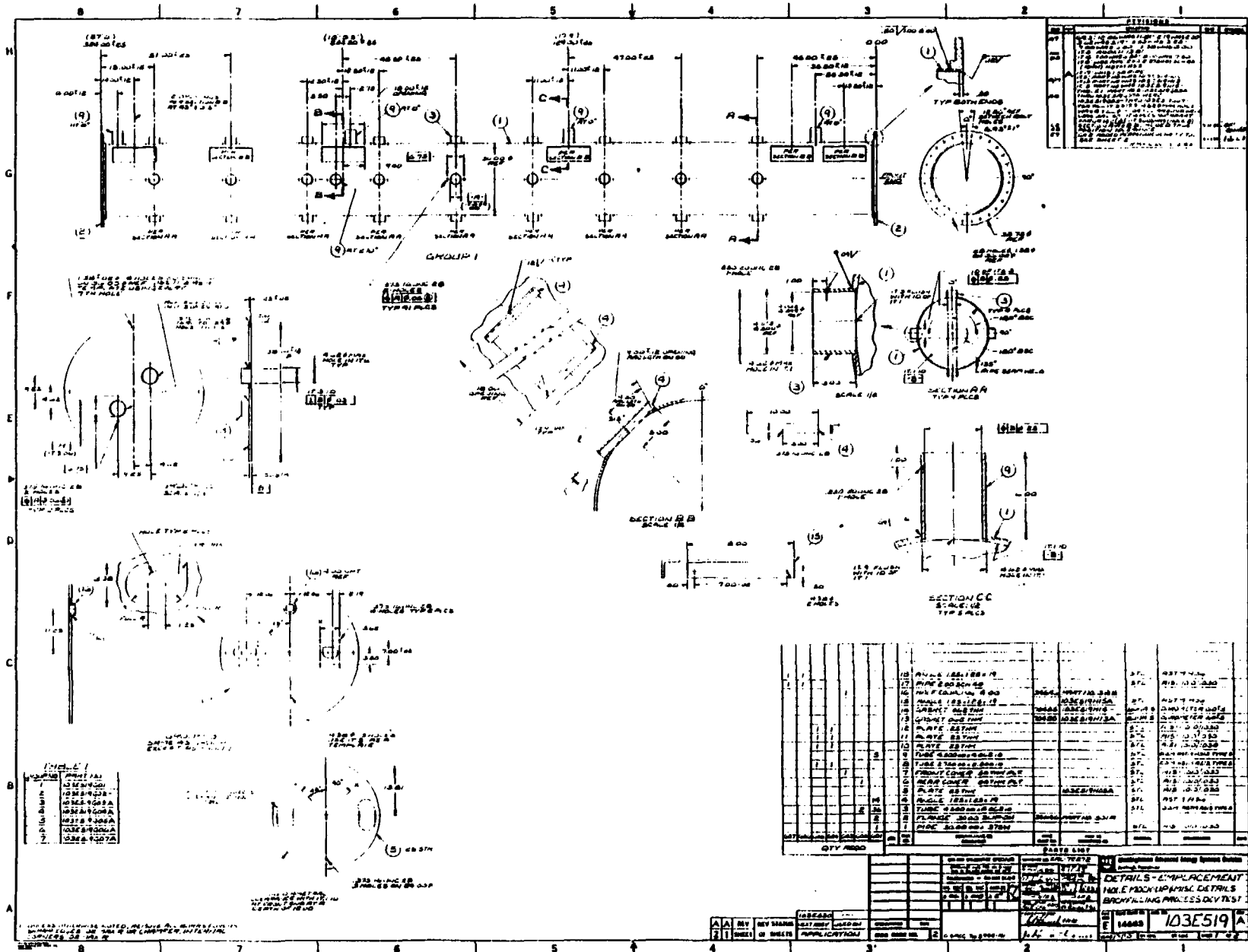
REV	DESCRIPTION	DATE
1	ISSUED FOR FABRICATION	10/15/53
2	REVISION	10/15/53
3	REVISION	10/15/53
4	REVISION	10/15/53
5	REVISION	10/15/53
6	REVISION	10/15/53
7	REVISION	10/15/53
8	REVISION	10/15/53
9	REVISION	10/15/53
10	REVISION	10/15/53
11	REVISION	10/15/53
12	REVISION	10/15/53
13	REVISION	10/15/53
14	REVISION	10/15/53
15	REVISION	10/15/53
16	REVISION	10/15/53
17	REVISION	10/15/53
18	REVISION	10/15/53
19	REVISION	10/15/53

REV	DESCRIPTION	DATE
1	ISSUED FOR FABRICATION	10/15/53
2	REVISION	10/15/53
3	REVISION	10/15/53
4	REVISION	10/15/53
5	REVISION	10/15/53
6	REVISION	10/15/53
7	REVISION	10/15/53
8	REVISION	10/15/53
9	REVISION	10/15/53
10	REVISION	10/15/53
11	REVISION	10/15/53
12	REVISION	10/15/53
13	REVISION	10/15/53
14	REVISION	10/15/53
15	REVISION	10/15/53
16	REVISION	10/15/53
17	REVISION	10/15/53
18	REVISION	10/15/53
19	REVISION	10/15/53

REV	DESCRIPTION	DATE
1	ISSUED FOR FABRICATION	10/15/53
2	REVISION	10/15/53
3	REVISION	10/15/53
4	REVISION	10/15/53
5	REVISION	10/15/53
6	REVISION	10/15/53
7	REVISION	10/15/53
8	REVISION	10/15/53
9	REVISION	10/15/53
10	REVISION	10/15/53
11	REVISION	10/15/53
12	REVISION	10/15/53
13	REVISION	10/15/53
14	REVISION	10/15/53
15	REVISION	10/15/53
16	REVISION	10/15/53
17	REVISION	10/15/53
18	REVISION	10/15/53
19	REVISION	10/15/53

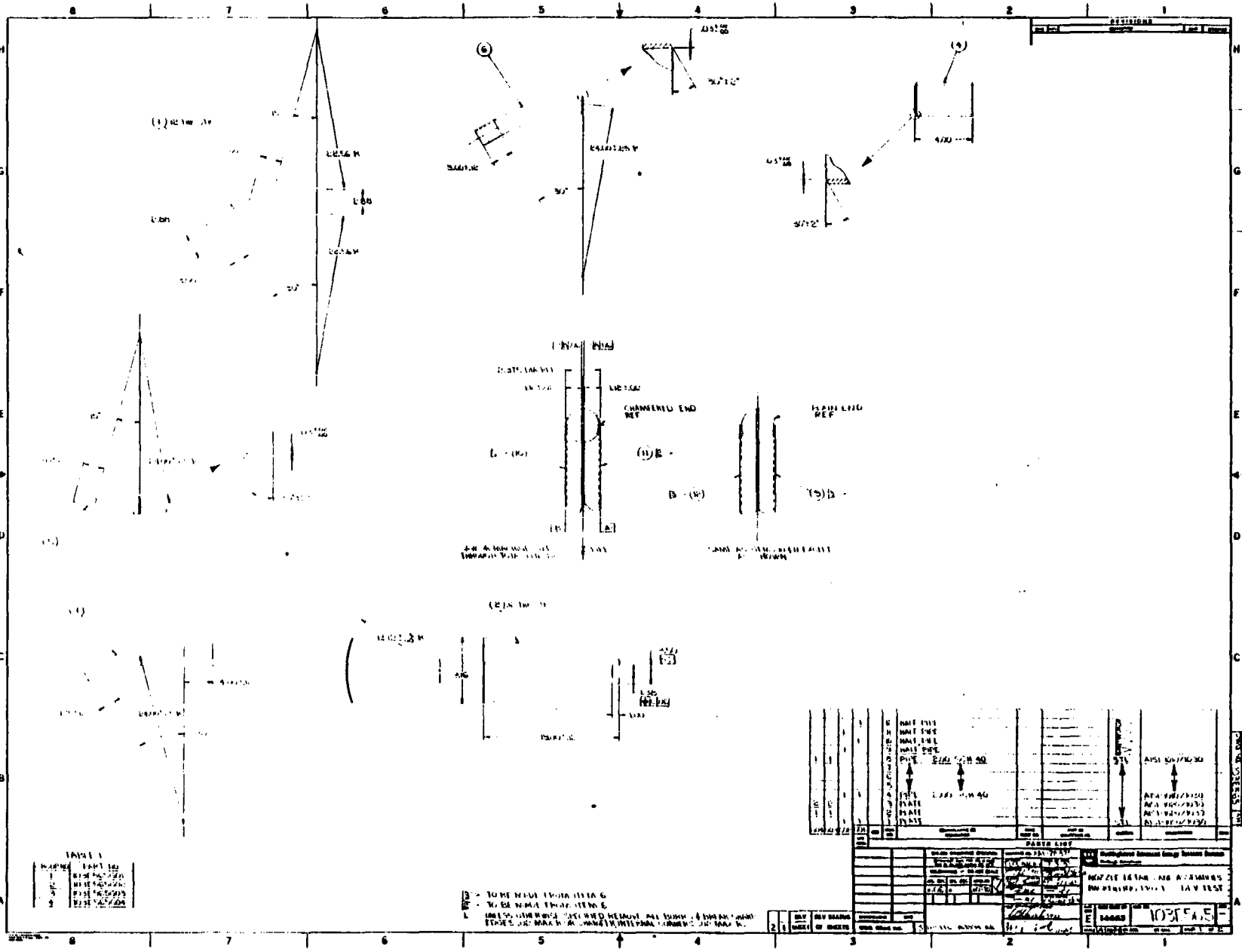
ALL DIMENSIONS ARE TO CENTERLINE UNLESS OTHERWISE SPECIFIED

DRAWING NO. 103513
 PART NO. 103513
 QUANTITY 1000
 DATE 10/15/53
 DRAWN BY [Signature]
 CHECKED BY [Signature]
 APPROVED BY [Signature]
 TITLE [Signature]
 MATERIAL [Signature]
 APPLICATION [Signature]

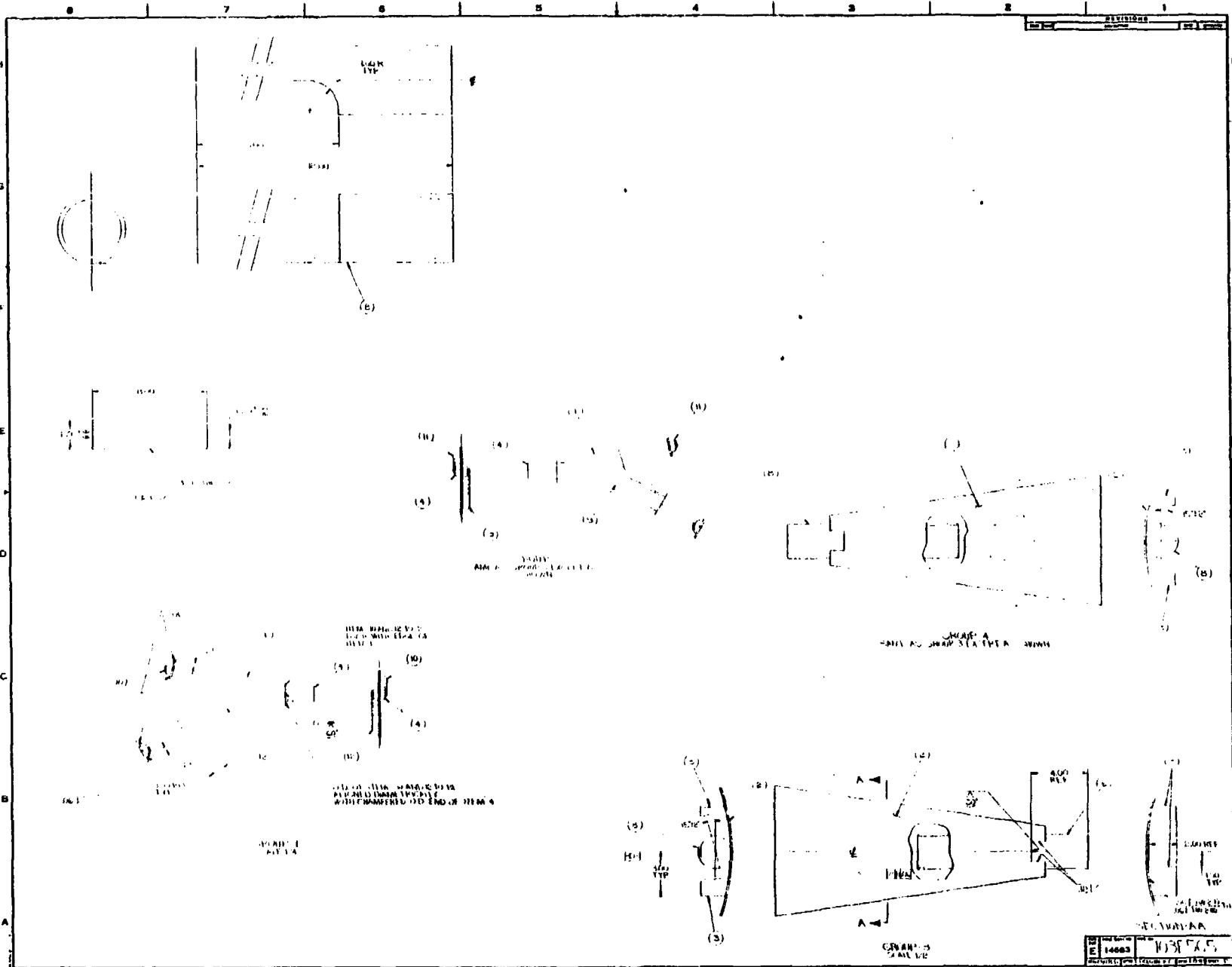


NO.	REVISION	DATE	BY	CHKD.
1				
2				
3				
4				
5				
6				
7				
8				
9				
10				
11				
12				
13				
14				
15				
16				
17				
18				
19				
20				
21				
22				
23				
24				
25				
26				
27				
28				
29				
30				
31				
32				
33				
34				
35				
36				
37				
38				
39				
40				
41				
42				
43				
44				
45				
46				
47				
48				
49				
50				

DATE	10/15/59	SCALE	AS SHOWN
PROJECT	103E519		
NO.	1	OF SHEETS	12
REV.	BY	DATE	
1			
2			
3			
4			
5			
6			
7			
8			
9			
10			
11			
12			
13			
14			
15			
16			
17			
18			
19			
20			
21			
22			
23			
24			
25			
26			
27			
28			
29			
30			
31			
32			
33			
34			
35			
36			
37			
38			
39			
40			
41			
42			
43			
44			
45			
46			
47			
48			
49			
50			



STEEL		CONCRETE		REINFORCING BARS	
1	A36	1	3000	1	A603
2	A36	2	3000	2	A603
3	A36	3	3000	3	A603
4	A36	4	3000	4	A603
5	A36	5	3000	5	A603
6	A36	6	3000	6	A603
7	A36	7	3000	7	A603
8	A36	8	3000	8	A603



APPENDIX B
ANALYSIS OF MIXTURES FOR BENTONITE TO BASALT RATIO

The purpose of the attached procedure is the quantitative separation of particulate bentonite from particulate basalt in a mixture of the two so that by comparison of weights before and after, the initial mass ratio of bentonite to basalt can be determined. It is desirable that this ratio be known within about $\pm 1\%$.

The general method of procedure requires extraction of bentonite by forming an aqueous sol, from which the basalt tends to settle, and siphoning off the unsettled upper portion. This operation is repeated until the residual bentonite is sufficiently attenuated to permit filtration of the solids from the remaining liquid. The solids, dried and weighed, represent the basalt fraction. An experimentally determined correction factor is applied to account for basalt fines lost in the processing, and the amount of bentonite is calculated as the difference between the sample weight and the corrected basalt weight.

The foregoing operations are imposed on a set of subsamples from each sample removed from the packing emplacement simulator after test. There are to be 43 such samples per test, of which 38 will comprise a volume of about one-liter each, and five will comprise about six liters each. It is suggested that three subsamples be drawn from each of the one-liter samples and five subsamples from each of the five liter samples. The enclosed procedure is written for 3 subsamples, but the adaptation to 5 subsamples is obvious. The minimum of subsamples per simulator run is thus 133.

- B.1 Materials and Equipment
 - B.1.1 Weighing vessels: Porcelain evaporating dishes or Petri dishes
 - B.1.2 One-liter plastic wide mouth bottles with screw caps
 - B.1.3 250 ml graduated cylinder
 - B.1.4 Flexible Tygon tubing, 1/4" ID, about 3 ft. long
 - B.1.5 Filtration assembly
 - B.1.5.1 Tubing and support manifold
 - B.1.5.2 Five receiver vessels
 - B.1.5.3 Five stoppers
 - B.1.5.4 Five Buchner funnels
 - B.1.6 Glass fiber filters (to fit Buchners), Whatman 934-AH
 - B.1.7 Plastic wash bottles, squeeze type
 - B.1.8 Brushes
 - B.1.9 Forceps
 - B.1.10 Scoop
 - B.1.11 Balance, 0.01g
 - B.1.12 One-liter volumetric flask
 - B.1.13 Calgon powder
 - B.1.14 Two-liter sample vessels, with covers
 - B.1.15 Labels

- B.2 Preparations**
- B.2.1** Obtain three samples. They will be stored in containers to be specified.
- B.2.2** Prepare three data sheets, one for each of the samples. Record sample ID, date, name of operator.
- B.2.3** Obtain a weighing vessel with a capacity of 150–200 cm³, and weigh it to the nearest 0.01g. Record the weight on each data sheet (line 2). NOTE: If you have access to an automatic taring balance, make a note to that effect and record the tare weight as 0.0.
- B.2.4** Obtain nine (9) evaporating dishes and number each consecutively, marking them on their unglazed bottoms. Be sure each is clean. Obtain a tare weight for each to the nearest 0.01 gram. Assign three (3) to each data sheet. Enter the tare weights along with the corresponding number of each on the data sheet (line 7).
- B.2.5** Obtain nine (9) one-liter plastic bottles with screw caps. Fill one with one-liter of water, using the one-liter volumetric flask. Make a horizontal mark at the waterline using a grease pencil. Make a second horizontal mark exactly 10 cm. below the first. Pour the water into a second bottle and repeat. Mark all the bottles in this way. Discard the water.
- B.2.6** Obtain four (4) additional one-liter plastic bottles with screw caps, and in each prepare one liter of Calgon solution by adding 50 ±1g of Calgon powder to each, and filling each with water. Cap and shake to dissolve powder. Label "Calgon Solution" and set aside.
- B.2.7** Set up the filtration assembly, and connect it to a vacuum system (pump or aspirator). Put a tubing clamp on each manifold side-tube. Place a glass fiber filter into each Buchner funnel.
- B.2.8** Set the vacuum oven to 95°C and turn on the heater power.

B.3 Subsample Preparation

- B.3.1** Place the sample into a covered plastic vessel with a capacity about twice the sample volume (the sample storage containers may be suitable).
- B.3.2** Shake the sample thoroughly to get uniform mixing of the basalt and bentonite components.
- B.3.3** Weigh about 100g of sample into the weighing dish, using the scoop. Any weight between 95 and 105g is suitable. Record the weight (line 1). NOTE: If you accidentally go over 105g do not try removing small amounts of material from the weighing dish; return the entire contents to the sample vessel and start over, at Step 3.2.
- B.3.4** Place the weighed sample into one of the empty one-liter bottles from step 2.4. Label or mark the bottle "[Sample ID]/Subsample No. []", inserting the indicated values.
- B.3.5** Repeat Steps 3.2 - 3.4 to obtain two more (total of three) subsamples.
- B.3.6** Repeat Steps 3.1 - 3.5 for a second and third sample, to provide a total of 9 subsamples to be run as a single analytical batch.
- B.3.7** Be sure there are entries on the data sheet for each subsample: weight of weighing vessel, weight of weighing vessel plus sample, weight of subsample (line 3). Be sure each plastic bottle is properly labeled.
- B.3.8** Set aside the three residual main samples in their containers until analysis is complete. Do not lose sample identity.

B.4 Dilution Procedure

- B.4.1** Using the 250 cm³ graduated cylinder, add 200 cm³ of Calgon solution to each of the plastic bottles containing subsamples.
- B.4.2** Fill each bottle to the liter mark with tapwater.
- B.4.3** Cap each bottle and shake each for exactly one minute. Let each bottle stand quietly for exactly 15 minutes.
- B.4.4** After 15 minutes, siphon off the supernatant liquid down to the lower mark, using the Tygon tubing. Discard the siphonate. NOTE: During siphoning move the siphon suction end slowly downward just under the liquid surface so that the lower levels of the solution undergo minimum disturbance.
- B.4.5** Add 100 cm³ of Calgon solution to each bottle and fill to the upper mark with water.
- B.4.6** Repeat Steps 4.3 - 4.5 five times (a total of 6 siphonings). Eliminate the Calgon solution addition after the fourth and subsequent siphonings, using only tapwater for refilling. Do not add water after the sixth (final) siphoning.

B.5 Filtration

- B.5.1** Introduce a vacuum in the vacuum manifold (pump or water aspirator). Release the clamp on one of the filter lines. Add, from a wash bottle, enough water to saturate the filter in each Buchner funnel and observe whether the suction is drawing properly. Label each funnel with the sample and subsample identity of one of the plastic bottles.
- B.5.2** Pour the contents of the chosen plastic bottle into one of the funnels and wash all solid material from the bottle using a stream of water from a wash bottle. Do not exceed the capacity of the receiver; change out the receiver if necessary.
- B.5.3** Repeat Steps 5.1 - 5.2 until all the manifolded filter stations are in use.
- B.5.4** After filtration is complete, wash the solid material in each funnel several times with small portions of water from a wash bottle. After the last washing allow the material to air dry with suction for a few minutes.
- B.5.5** Clamp the hose on a filter station for which Step 5.4 is complete, and break the vacuum. Lift out the Buchner funnel and, using forceps and brush, transfer its contents, including filter, into one of the previously tared evaporating dishes (Step 2.4). Perform this operation over a clean sheet of paper so that material accidentally spilled can be returned to the weighing vessel. Assign that dish and its tare weight to the space on the data sheet corresponding to the subsample just filtered.
- B.5.6** Repeat 5.5 for all the samples in the filter manifold. Set the filled evaporating dishes aside.
- B.5.7** Wash all the Buchner funnels to remove any residues and discard the filtrates. Set up the manifold once again as in 2.7.
- B.5.8** Repeat Steps 5.1 - 5.7 until all samples have been filtered.

B.6 Drying and Weighing

- B.6.1** Place the nine evaporating dishes containing moist solids into a vacuum oven heated to 95°C (Step 2.8). Start the pump, open the pump valve and close the vent valve. Close door and hold until vacuum gauge shows a pressure differential. Leave vessels for a minimum of 3 hours; overnight is acceptable.
- B.6.2** Remove the weighing vessels from the oven and allow them to cool to room temperature.
- B.6.3** Weigh each vessel and record the weight on the data sheet (line 4).
- B.6.4** Discard contents of the weighing vessels.

B.7 Calculations

- B.7.1 Subtract line 2 from line 1 and place the result in line 3. This gives the original subsample weight.**
- B.7.2 Subtract line 5 from line 4 and place the result in line 6. This corrects for the weight of the filter.**
- B.7.3 Subtract line 7 from line 6 and place the result in line 8. This gives the weight of basalt recovered.**
- B.7.4 Adjust the recovered basalt weight to 100g of charge by multiplying line 8 by the factor (100/line 3). Place the result in line 9.**
- B.7.5 Add the correction factor in line 10 to line 9 and place the results in line 11. This gives the corrected weight of basalt recovered.**
- B.7.6 Subtract line 11 from line 3, and place the result in line 12. This gives the amount of bentonite in the original sample.**
- B.7.7 Divide line 12 by line 11 and place the results in line 13. This gives the bentonite/basalt ratio.**
- B.7.8 Average the results in line 13, and place the average in line 14. Place the standard deviation in line 15.**

DATE: _____

SAMPLE ID _____

OPERATOR: _____

ANALYSIS OF MIXTURES FOR BENTONITE BASALT RATIO

Sub-Sample Number:	1	2	3	4	5
1. Weight: Weighing Vessel + Sub-sample					
2. Weight: Weighing Vessel					
3. Weight: Sub-sample					
4. Weight: Evaporating Dish + Solids + Filter					
5. Weight Filter	0.63	0.63	0.63	0.63	0.63
6. Weight: Evaporating Dish + Solids					
7. Weight: Evaporating Dish					
8. Weight Solids					
9. Adjusted Basalt Weight					
10. Correction Factor	1.16	1.16	1.16	1.16	1.16
11. Corrected Basalt Weight					
12. Bentonite Weight, Calculated					
13. Ratio, Bentonite/Basalt					
14. Ratio, Bentonite/Basalt, Average					
15. Standard Deviation of Ratio					

COMMENTS:

Signed: _____

Date: _____

Checked: _____

Date: _____

MTSD-TME-030
DRAFT

APPENDIX C DATA AND ANALYSIS

C.1 METHODOLOGY

In analyzing the data on the mixture (basalt-to-bentonite) homogeneity of the packed material the measurement of interest is the percentage of basalt in the mixture as a function of position in the borehole simulator; a high degree of homogeneity would be indicated by minimal variation in this quantity. Other measurables, such as percent bentonite or basalt-to-bentonite ratio, would also serve, but percent basalt is convenient. Since in deriving this measurement, a large number of samples is taken from various places in the simulator, and subsamples of these are ultimately analyzed, the results will reflect some combination of variability arising from location, sampling, and subsampling/analysis. To separate the total variability into parts assignable to these various sources, the so-called hierarchal, or nested, statistical model was invoked (Reference 4).

If η is the true mean of the basalt concentration, the overall error, ϵ , will contain three separate components: $\epsilon = \epsilon_a + \epsilon_s + \epsilon_b$, where ϵ_a is the error in analysis, ϵ_s is the error associated with sampling, and ϵ_b is the batch error, for our purposes in this application, the error associated with some gross portion of the emplaced packing, such as top vs bottom, or right side vs left side. We assume these errors all have zero means, and that they represent samples from normal distributions having variances σ_a , σ_s , and σ_b . Thus a measurement on each single sample would have a total variability related in some way to these three component variances. But only the batch-to-batch variance is critical in determining the large scale homogeneity of the emplaced packing; sampling errors and analytical errors inflate the overall variance randomly, and are, effectively for this purpose, mere noise. The hierarchal model was therefore invoked in the analysis to resolve the overall variance into its components so that a statistically sound decision could be formally rendered on the credibility of the null hypothesis, namely, to accept or reject the proposition that there is no difference between the true basalt concentration mean of this region (batch 1) as compared with that of that region (batch 2) in the simulator. A pictorial representation of the situation is given in Figure 18.

For the homogeneity relationships considered here, the hierarchal design is made up of 2 "batches", 18 samples per batch, and 3 analyses per sample, ie, a $2 \times 18 \times 3$ design. Thus, a total of 108 analytical measurements was made for each test series. For each separate test of hypothesis contrasting differing parts of the simulator, the data were redistributed to fit the contrast under consideration. Calculations were performed using the computer program HIERARC2, written for this purpose. A listing of the computer program and sample output are presented in Appendix E. This program was written for the IBM PC.

Density data were handled in a simpler fashion; since there is only one determination per sample, the design above devolves into a two-level (2×18) design, which is better handled by a simple Student's t-test based on the average for each set of 18 measurements. Again, the same data were redistributed for the calculation of each contrast considered.

Other statistical assessments of the data were carried out using the statistical computer program PC Statistician, written for the IBM PC by Human Systems Dynamics.

C.2 DENSITY

The density data for all four test series are presented in Table 1. As indicated earlier, the densities from the first two series, because of inconsistencies and irregularities in test operation, are not regarded as equivalent to the data from series 3 and 4, to which the full analysis was applied. The sample average analysis, whose results are presented in Tables 2

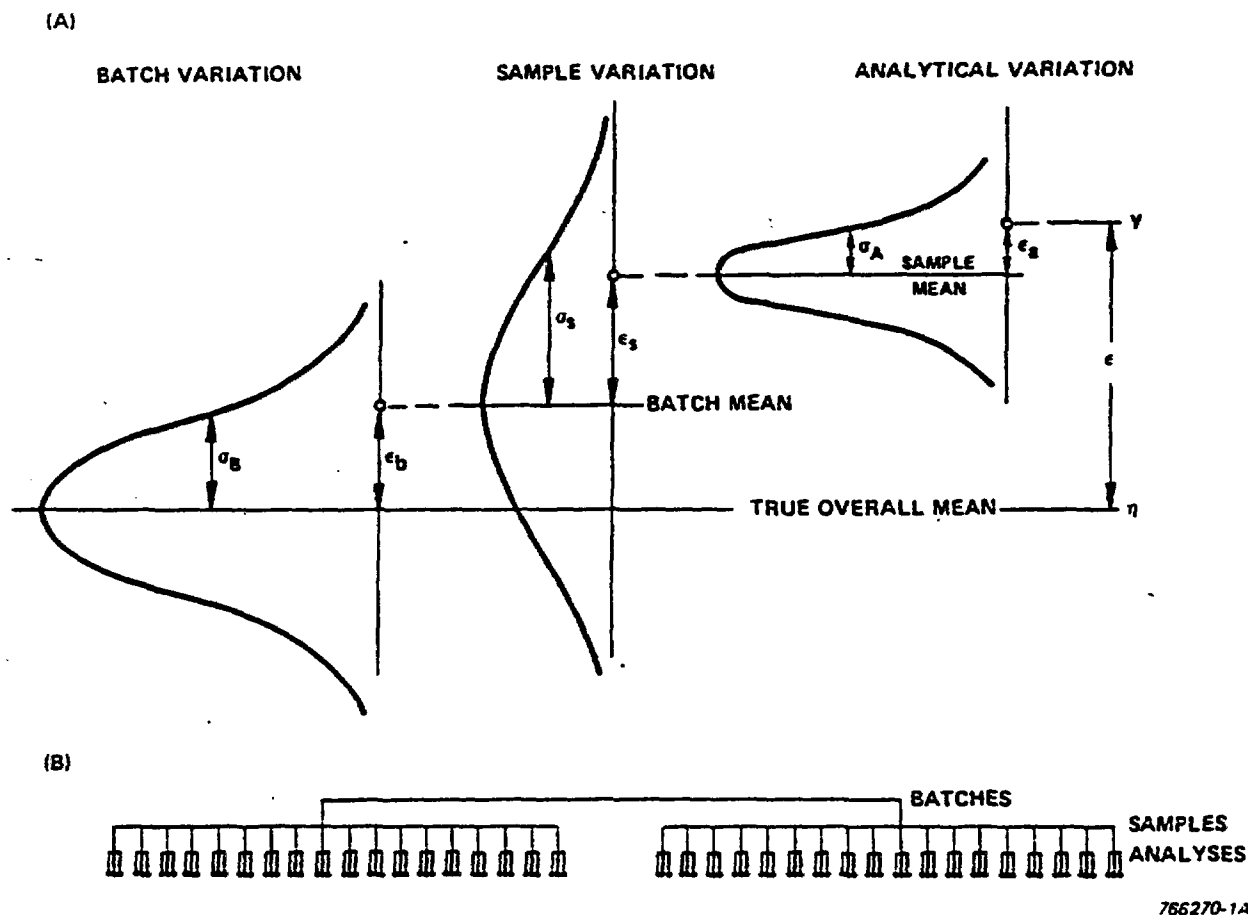


Figure 18

(A) Resolution of variances. y , the result of a single measurement, differs from μ , the true mean, by error ϵ , which is the sum of the three errors shown, $\epsilon_b + \epsilon_s + \epsilon_a$. Each of these component errors is the deviation from the mean of the conceptual population that might have been obtained from the single observation at the next higher level, e.g., the conceptual population of analytical results that might have been obtained by analysis of a single sample. These conceptual populations are assumed to be normally distributed with the variances shown, and the hierarchical design calculations are able to resolve these variances.

(B) A 2 x 18 x 3 hierarchical design.

TABLE 1. Density Data, Runs 1 through 4

<u>SAMPLING POSITION</u>	<u>QUAORANT</u>	<u>SERIES</u>			
		<u>1</u>	<u>2</u>	<u>3</u>	<u>4</u>
A	-	1.42	1.53	1.70	1.64
A	-	1.53	1.75	1.66	1.75
B	-	1.39	1.57	1.54	1.57
C	1	1.43	1.60	1.60	1.61
D	1	1.48	-	1.66	1.66
E	1	1.50	-	1.66	1.57
G	-	1.35	-	1.40	1.44
H	1	1.38	-	1.62	1.63
J	1	1.64	-	1.82	1.68
K	1	1.39	-	1.63	1.62
L	-	1.19	-	1.32	1.43
M	1	1.36	-	1.62	1.77
N	1	1.42	-	1.57	1.66
P	1	1.36	-	1.64	1.71
R	-	1.14	-	1.39	1.47
C	4	1.30	1.75	1.73	1.59
D	4	1.26	-	1.77	1.56
E	4	1.36	-	1.62	1.64
F	-	1.22	-	1.39	1.36
H	4	1.23	-	1.60	1.59
J	4	1.40	-	1.68	1.64
K	4	1.38	-	1.58	1.57
M	4	1.41	-	1.59	1.61
N	4	1.42	-	1.62	1.66
P	4	1.32	-	1.66	1.63
C	3	1.46	1.65	1.65	1.60
D	3	1.56	1.58	1.61	1.47
E	3	1.44	-	1.47	1.42
H	3	1.43	-	1.40	1.43

1283I:25-51

TABLE 1. DENSITY DATA, RUNS 1 THROUGH 4 (Continued)

<u>SAMPLING POSITION</u>	<u>QUADRANT</u>	<u>SERIES</u>			
		<u>1</u>	<u>2</u>	<u>3</u>	<u>4</u>
J	3	1.40	-	1.34	1.51
K	3	1.34	-	1.48	1.66
M	3	1.51	-	1.53	1.52
N	3	1.46	-	1.46	1.55
P	3	1.40	-	1.43	1.60
C	2	1.40	1.64	1.59	1.59
D	2	1.45	1.52	1.51	1.43
E	2	1.36	-	1.55	1.34
H	2	1.36	-	1.48	1.39
J	2	1.41	-	1.32	1.43
K	2	1.46	-	1.37	1.50
M	2	1.50	-	1.39	1.53
N	2	1.40	-	1.33	1.42
P	2	1.43	-	1.37	1.51

NOTE: Letters ascend from A at the inert end of the simulators. Facing in the letters-ascending direction, quadrants run 1, 2, 3, 4 counter clockwise, 1 and 4 being upper quadrants, 1 and 2, being left-hand quadrants.

TABLE 2. ANALYSIS OF DENSITY DATA, RUN 1 (g/cc)

	<u>AVG</u>	<u>STD DEV</u>	<u>STD ERR</u>	<u>VAR</u>	<u>POOLED VAR</u>
Overall	1.398	0.095	0.01	0.0090	---
Short tube average	1.413	0.077	0.01	0.0059	---
Top average (1,4)	1.391	0.092	0.02	0.0085	0.0056
Bottom average (2,3)	1.435	0.052	0.01	0.0027	---
Right average (1,2)	1.430	0.070	0.02	0.0049	0.0058
Left average (3,4)	1.396	0.082	0.02	0.0069	---
Front average (K,M,N,P)	1.414	0.051	0.01	0.0026	0.0057
Back average (C,D,E,H)	1.412	0.094	0.02	0.0088	---
Upper right (1)	1.44	0.090	0.03	0.0081	
Lower right (2)	1.42	0.047	0.02	0.0022	
Lower left (3)	1.45	0.056	0.02	0.0031	
Upper left (4)	1.34	0.068	0.02	0.0046	

DATA COMPARISONS:

	<u>PLD VAR</u>	<u>OBS DIFF</u>	<u>DEGS OF FREEDOM</u>	<u>CALCD t</u>	<u>TAB t</u>	<u>DIFF SGNFCNT?</u>
Top/bottom	0.0056	0.044	34	1.76	2.034	no
Right/left	0.0058	0.034	34	1.34	2.034	no
Front/back	0.0057	0.002	30	0.079	1.946	no

Load Cell Density: 1.37

95% Confidence Interval for the true density: Prob $[1.391 \leq \eta \leq 1.435] = 0.95$

TABLE 2. ANALYSIS OF DENSITY DATA, RUN 3 (g/cc)

	<u>AVG</u>	<u>STD DEV</u>	<u>STD ERR</u>	<u>VAR</u>	<u>POOLED VAR</u>
Overall	1.543	0.131	0.02	0.0172	---
Short tube average	1.554	0.127	0.02	0.0161	---
Top average (1,4)	1.648	0.066	0.02	0.0044	0.0072
Bottom average (2,3)	1.460	0.100	0.02	0.0137	---
Right average (1,2)	1.540	0.138	0.03	0.0190	0.0150
Left average (3,4)	1.568	0.117	0.03	0.0137	---
Front average (K,M,N,P)	1.517	0.112	0.03	0.0125	0.0150
Back average (C,D,E,H)	1.584	0.132	0.03	0.0174	---
Upper right (1)	1.65	0.07	0.02	0.0050	
Lower right (2)	1.43	0.10	0.02	0.010	
Lower left (3)	1.49	0.10	0.02	0.010	
Upper left (4)	1.65	0.07	0.02	0.0050	

DATA COMPARISONS:

	<u>PLD VAR</u>	<u>OBS DIFF</u>	<u>DEGS OF FREEDOM</u>	<u>CALCD t</u>	<u>TAB t</u>	<u>DIFF SGNFCNT?</u>
Top/bottom	0.0072	0.188	34	6.68	2.034	yes
Right/left	0.00164	0.028	34	0.639	2.034	no
Front/back	0.00150	0.067	30	1.12	1.946	yes (borderline)

Load Cell Density: 1.56

95% Confidence Interval for the true density: Prob $[1.518 \leq \eta \leq 1.590] = 0.95$

TABLE 2. ANALYSIS OF DENSITY DATA, RUN 4 (g/cc)

	<u>AVG</u>	<u>STD DEV</u>	<u>STD ERR</u>	<u>VAR</u>	<u>POOLED VAR</u>
Overall	1.557	0.105	0.016	0.11	---
Short tube average	1.564	0.099	0.016	0.00984	---
Top average (1,4)	1.633	0.053	0.00880	0.00279	0.00501
Bottom average (2,3)	1.494	0.0851	0.0142	0.00724	---
Right average (1,2)	1.558	0.121	0.0202	0.0147	0.0101
Left average (3,4)	1.569	0.0738	0.0123	0.00545	---
Front average (K,M,N,P)	1.595	0.0887	0.0222	0.00787	0.00965
Back average (C,D,E,H)	1.532	0.102	0.0254	0.0103	---
Upper right (1)	1.663	0.0685	0.0228	0.00469	
Lower right (2)	1.460	0.0779	0.0260	0.00607	
Lower left (3)	1.529	0.0816	0.0272	0.00666	
Upper left (4)	1.610	0.0346	0.0115	0.00120	

DATA COMPARISONS:

	<u>PLD VAR</u>	<u>OBS DIFF</u>	<u>DEGS OF FREEDOM</u>	<u>CALCD t</u>	<u>TAB t</u>	<u>DIFF SGNFCNT?</u>
Top/bottom	0.00502	0.1389	34	5.88	2.034	yes
Right/left	0.0101	0.0111	34	0.332	2.034	no
Front/back	0.00965	0.0656	30	1.89	1.946	no
Series 3/4	0.130	0.100	70	0.373	1.997	no

Load Cell Density: 1.59

95% Confidence Interval for the true density: Prob [1.536 \leq ρ \leq 1.592] = 0.95

TABLE 3. DENSITY CROSS TABULATIONS

Cross Tabulation File name: BACKFIL3

POSITION VS DENSITY, RUN 3

Records read: 36
Missing data: 0
Unclassifiables: 0

Classification scheme

DIST : 0 - 2.5 2.6 - 5 5.1 - 8

DENS : 0 - 1.4 1.41 - 1.45 1.46 - 1.5 1.51 - 1.55 1.56 - 1.6 1.61 - 1.65 1.66 - 1.7 1.71 - 2

Cross Tabulation File name: BACKFIL3

QUADRANTS VS DENSITY

Records read: 36
Missing data: 0
Unclassifiables: 0

Classification scheme

QUAD : 1 2 3 4

DENS : 0 - 1.4 1.41 - 1.45 1.46 - 1.5 1.51 - 1.55 1.56 - 1.6 1.61 - 1.65 1.66 - 1.7 1.71 - 2

73

P O S I T I O N		DENSITY, G/CC								total
		1	2	3	4	5	6	7	8	
	BACK	0	0	1	2	2	3	2	2	12
	CENTE	4	0	2	0	2	2	1	1	12
	FRONT	3	1	1	1	2	3	1	0	12
	total	7	1	4	3	6	8	4	3	36

Q U A D R A N T S		DENSITY, G/CC								total
		1	2	3	4	5	6	7	8	
	1ST	0	0	0	0	2	4	2	1	9
	2ND	3	0	1	2	1	0	0	0	9
	3RD	2	1	3	1	0	2	0	0	9
	4TH	0	0	0	0	3	2	2	2	9
	total	7	1	4	3	6	8	4	3	36

HTSD-THE-030
DRAFT

TABLE 3. DENSITY CROSS TABULATIONS (Continued)

Cross Tabulation File name: BACKFILE

POSITION VS DENSITY, RUN 4

Records read: 36
Missing data: 0
Unclassifiable: 0

Classification scheme

DIST : 0 - 2.5 2.6 - 5 5.1 - 8

DENS : 0 - 1.4 1.41 - 1.45 1.46 - 1.5 1.51 - 1.55 1.56 - 1.6 1.61 - 1.65 1.66 - 1.7 1.71 - 2

Cross Tabulation File name: BACKFILE

QUADRANTS VS DENSITY, RUN 4

Records read: 36
Missing data: 0
Unclassifiable: 0

Classification scheme

QUAD : 1 2 3 4

DENS : 0 - 1.4 1.41 - 1.45 1.46 - 1.5 1.51 - 1.55 1.56 - 1.6 1.61 - 1.65 1.66 - 1.7 1.71 - 2

74

P		DENSITY, G/CC								total
		1	2	3	4	5	6	7	8	
B	BACK	1	2	1	0	5	2	1	0	12
I	CENTE	1	2	1	1	2	3	2	0	12
N	FRONT	0	1	0	4	1	2	2	2	12
	total	2	5	2	5	8	7	5	2	36

Q		DENSITY, G/CC								total
		1	2	3	4	5	6	7	8	
B	1ST	0	0	0	0	1	3	3	2	9
A	2ND	2	3	1	2	1	0	0	0	9
N	3RD	0	2	1	3	2	0	1	0	9
S	4TH	0	0	0	0	4	4	1	0	9
	total	2	5	2	5	8	7	5	2	36

HTSD-TRE-030
DRAFT

and 3, shows that in both tests, the mean density was the same, about 1.56 g/cc, or 57.8% percent theoretical. On the other hand, the overall densities for the two tests, calculated from the total mass deposited and the simulator volume, were 1.56 and 1.59. These figures, when compared to the results from the first test, 1.41 from the sample average and 1.37 from the load cells, show a significant gain, but when compared with the desired 70% theoretical show a long way to go. In the figures above the sample average is considered somewhat more reliable, because, although the load cell readings are highly precise, the presence of voids, some observed and others possible, makes the true filled simulator volume uncertain. Of course a similar bias could exist in the volume of each sample cylinder, but since their number is large, and the associated biases can be of either sign, averaging will tend to cancel out any effect.

Density data are separated into contributions from the four quadrants in Table 2, which also presents the results of the Student's t analysis of the density homogeneity. The results show that while there is no significant difference in density in either test from side to side or from front to back of the simulator, in both tests there is a significant difference from top to bottom: the mean density in the top half is significantly greater than that in the bottom half. "Significant" is used here in the statistical sense: at the 95% confidence level, we believe that this result is not simply due to chance. This result is also evident in the cross tabulations presented in Table 3, where it is obvious that the the densities in the first and fourth quadrants, the upper ones, contained only the higher density groups (those numbered 5-8), while the lower quadrants contained dominantly the lower density groups.

The general frequency distribution for density is presented in Figures 12 and 13. These figures show that while the bulk of the samples had densities in the range about the average, from 1.52 to 1.65 g/cc, the full range of the data extended from 1.32 to 1.82 g/cc. The latter figure is about 67% theoretical, and suggests that, since at least one region, between the two tests, achieved that level, its attainment as an overall average is, at the very least, a practical possibility.

C.3 MINERAL HOMOGENEITY

The basalt concentrations measured in series 3 and 4 are presented in Table 4 and the results of analysis appear in Tables 5 and 6. The mean basalt concentration was close to the target value of 75% basalt in both tests; specifically, the grand average of all samples for test 3 was 74.13%, and for test 4 was 75.20%. The frequency distributions for the basalt concentrations in the two tests are given in Figs 14 and 15, where it can be seen that the overall homogeneity spread is reasonably narrow, especially in test 4, and concentrated in a band between 70 and 80 percent. This is also shown in the cross-tabulation of Table 6, where it can be seen that except for the four VL (very low) sports in test 3, the bulk of the data lines up in the ML, M, and MH bands.

The cross tabulation for quadrants in run 4 (Table 6) suggests that the basalt concentration is generally higher in the two upper quadrants, 1 and 4, than it is in the lower quadrants. The computer runs using the HIERARC2 computer program confirm this inhomogeneity; the output for this particular case is included in Appendix E, and is summarized in part of Table 5. The difference is statistically significant, and cannot be reasonably explained as a result of random error. This difference is the only large scale homogeneity detected by HIERARC2 in any of the six studies made (for each test, a contrast of top-to-bottom, side-to side, and front-to-back).

However, the computer program consistently, in all six runs, indicated that the dominant component of test variance is associated with the sampling, one sample being associated with each of the 36 short sampling cylinders. The significance of this finding is that there is a mid-scale graininess in the inhomogeneity developed by the emplacement configuration used: The averaging of the sample basalt concentration produces reasonably low variability when large, several ton, "batches" are contrasted (notwithstanding the top-to-bottom inhomogeneity discussed above; even in that case the sample variance was dominant), and the analysis of sub-samples, three of which were extracted from each sample, also produced a reasonably low variability; both variabilities are low in comparison with the sample variability. Thus the emplaced packing is characterized by a kind of "clumped" inhomogeneity, and from the size of the sampling cylinders and their relative placement in the simulator tube, we can guess the "clump" size to be from a few liters to a few tens of liters.

TABLE 4. BASALT CONCENTRATION DATA

SAMPLING POSITION	QUADRANT	SERIES 3			SERIES 4		
		1	2	3	1	2	3
A	-	89.59	90.68	86.36	85.35	81.60	93.32
A	-	75.07	77.58	79.47	78.16	86.77	83.87
B	-	74.62	79.33	81.14	-	-	-
C	1	83.70	81.87	83.43	80.19	75.08	77.89
D	1	75.81	82.30	88.06	73.85	83.44	76.11
E	1	69.98	75.80	69.74	69.42	72.85	64.45
G	-	-	-	-	-	-	-
H	1	81.38	74.77	76.59	84.00	85.05	80.79
J	1	69.79	69.93	71.22	84.50	77.61	80.39
K	1	60.34	59.66	61.52	75.30	77.30	69.82
L	-	79.76	82.65	81.27	-	-	-
M	1	71.66	76.50	74.76	75.42	78.89	74.17
N	1	67.05	71.38	69.32	88.42	84.07	87.61
P	1	72.70	74.96	73.83	78.29	75.08	78.40
C	3	86.83	85.54	77.37	83.56	84.58	85.09
R	-	71.57	75.03	73.76	-	-	-
C	4	71.71	70.60	73.22	73.64	76.31	82.78
D	4	79.76	78.30	78.54	73.12	81.41	75.91
E	4	67.04	69.65	67.61	75.42	69.83	69.59
F	-	-	-	-	-	-	-
H	4	75.90	74.18	76.60	78.02	79.61	78.59
J	4	70.14	76.82	71.24	81.97	72.84	78.82
K	4	60.70	62.15	61.42	74.48	69.92	82.37
M	4	75.33	80.04	76.49	83.22	86.67	76.42
N	4	69.30	71.04	71.13	81.86	80.59	82.75
P	4	76.51	75.10	75.83	72.29	72.29	77.28
C	3	86.83	85.54	77.37	83.56	84.58	85.09
D	3	74.34	70.22	68.54	73.22	72.37	70.50
E	3	60.76	62.26	61.38	76.77	71.57	78.12
H	3	53.49	50.45	51.60	75.84	70.35	77.31

12831:25-58

TABLE 4. BASALT CONCENTRATION DATA (Continued)

<u>SAMPLING POSITION</u>	<u>QUADRANT</u>	<u>SERIES 3</u>			<u>SERIES 4</u>		
		<u>1</u>	<u>2</u>	<u>3</u>	<u>1</u>	<u>2</u>	<u>3</u>
J	3	73.42	72.83	71.69	75.26	72.45	69.34
K	3	86.91	91.52	82.24	78.49	74.92	73.04
M	3	79.19	85.10	82.62	67.51	69.45	68.38
N	3	78.45	80.06	81.89	76.62	72.73	74.19
P	3	74.86	77.96	82.28	74.63	76.53	76.48
C	2	77.07	75.52	75.17	80.37	78.55	78.19
D	2	76.03	76.79	76.03	68.84	66.15	66.62
E	2	75.12	79.45	79.30	74.42	71.64	71.50
H	2	71.26	76.25	69.78	73.77	74.58	76.94
J	2	71.51	71.04	71.94	66.43	64.50	66.17
K	2	80.23	81.93	81.08	73.46	70.54	69.52
M	2	74.35	73.71	76.73	69.49	68.95	65.10
N	2	74.71	79.19	77.94	65.23	68.95	68.95
P	2	76.28	75.72	76.29	68.87	69.58	69.35

See note after Table 1

TABLE 5. BASALT CONCENTRATION ANALYSIS

SERIES 3:

GENERAL: Grand average = 74.13

Std. deviation of y = 7.32

Std. error of y-bar = 0.70

95% Confidence statement:

Prob [72.74 < True mean < 75.52] = 0.95

ESTIMATE OF VARIANCE

	<u>Analytical</u>	<u>Samples</u>	<u>Batches</u>
Top/bottom	7.70	47.24	0.0
Left/right	7.70	47.53	0.0
Front/back	7.70	47.82	0.0

	<u>BATCH/SAMPLES F-RATIO</u>			<u>SAMPLES/ANALYSIS F-RATIO</u>		
	<u>DF</u>	<u>Calcd</u>	<u>Tab</u>	<u>DF</u>	<u>Calcd</u>	<u>Tab</u>
Top/bottom	1,34	0.646	4.13	34,72	19.41	2.02
Left/right	1,34	0.443	4.13	34,72	19.52	2.02
Front/back	1,34	0.249	4.13	34,72	19.63	2.02

	<u>MEAN, m</u>		<u>DELTA</u> <u>m</u>	<u>t-calc</u>	<u>DF</u>	<u>2-TAIL</u> <u>PROB</u>	<u>DIFF</u> <u>SGNFCNT?</u>
	<u>Batch 1</u>	<u>Batch 2</u>					
Top/bottom	73.19	75.08	-1.89	0.803	34	0.432	no
Left/right	74.92	73.35	1.57	0.665	34	0.482	no
Front/back	73.54	74.72	-1.18	0.499	34	0.374	no

TABLE 5. BASALT CONCENTRATION ANALYSIS (Continued)

SERIES 4:

GENERAL: Grand average = 75.21

Std. deviation of y = 5.61

Std. error of y-bar = 0.54

95% Confidence statement:

Prob [74.13 < True mean < 76.59] = 0.95

ESTIMATE OF VARIANCE

	<u>Analytical</u>	<u>Samples</u>	<u>Batches</u>				
Top/bottom	8.91	17.1	11.4				
Left/right	8.91	23.0	0.0165				
Front/back	8.66	22.6	0.0				
	<u>BATCH/SAMPLES F-RATIO</u>			<u>SAMPLES/ANALYSIS F-RATIO</u>			
	<u>DF</u>	<u>Calcd</u>	<u>Tab</u>	<u>DF</u>	<u>Calcd</u>	<u>Tab</u>	
Top/bottom	1,34	11.23	4.13	34,72	6.77	2.01	
Left/right	1,34	1.01	4.13	34,72	8.75	2.01	
Front/back	1,30	0.268	4.17	30,64	8.82	2.02	
	<u>MEAN, m</u>		<u>DELTA</u>	<u>t-calc</u>	<u>DF</u>	<u>2-TAIL</u>	<u>DIFF</u>
	<u>Batch 1</u>	<u>Batch 2</u>	<u>m</u>			<u>PROB</u>	<u>SGNFCNT?</u>
Top/bottom	77.71	72.70	5.01	3.35	34	0.00232	yes
Left/right	74.35	76.06	-1.71	1.01	34	0.322	no
Front/back	75.80	74.87	0.923	0.518	30	0.286	no

TABLE 6. BASALT CONCENTRATION CROSS TABULATIONS

Cross Tabulation File name: BACKFIL3

POSITION VS BASALT CONCENTRATION, RUN 3

Records read: 36
Missing data: 0
Unclassifiables: 0

Classification scheme

BIST : 0 - 2.5 2.6 - 5 5.1 - 8

BASALG: 0 - 62.5 62.51 - 67.5 67.51 - 72.5 72.51 - 77.5 77.51 - 82.5
82.51 - 87.5 87.51 - 100

Cross Tabulation File name: BACKFIL3

QUADRANTS VS BASALT CONCN, RUN 3

Records read: 36
Missing data: 0
Unclassifiables: 0

Classification scheme

QUAD : 1 2 3 4

BASALG: 0 - 62.5 62.51 - 67.5 67.51 - 72.5 72.51 - 77.5 77.51 - 82.5
82.51 - 87.5 87.51 - 100

P O S I T I O N		BASALT CONCN, %							total
		VL	L	ML	H	MH	H	VH	
	BACK	1	0	3	3	3	2	0	12
	CENTE	3	0	4	3	1	1	0	12
	FRONT	0	0	2	7	3	0	0	12
	total	4	0	9	13	7	3	0	36

Q U A D R A N T S		BASALT CONCN, %							total
		VL	L	ML	H	MH	H	VH	
	1ST	1	0	3	3	1	1	0	9
	2ND	0	0	2	5	2	0	0	9
	3RD	2	0	1	1	3	2	0	9
	4TH	1	0	3	4	1	0	0	9
	total	4	0	9	13	7	3	0	36

TABLE 6. BASALT CONCENTRATION CROSS TABULATIONS (Continued)

Cross Tabulation File name: BACKFIL4

POSITION VS BASALT CONCENTRATION, RUN 4

Records read: 36
Missing data: 0
Unclassifiable: 0

Classification scheme

BIST : 0 - 2.5 2.6 - 5 5.1 - 10

BASAVG: 0 - 42.5 42.51 - 47.5 47.51 - 72.5 72.51 - 77.5 77.51 - 82.5
82.51 - 87.5 87.51 - 100

Cross Tabulation File name: BACKFIL4

QUADRANTS VS BASALT CONC, RUN 4

Records read: 36
Missing data: 0
Unclassifiable: 2

Classification scheme

QUAD : 1 2 3 4

BASAVG: 0 - 42.5 42.51 - 47.5 47.51 - 72.5 72.51 - 77.5 77.51 - 82.5 82.51 -
87.5 87.51 - 100

P O S I T I O N		BASALT CONC, 1							total
		VL	L	ML	M	HW	H	VW	
	BACK	0	1	3	3	4	1	0	12
	CENTE	0	1	2	5	3	1	0	12
	FRONT	0	0	4	5	2	1	0	12
	total	0	2	9	13	9	3	0	36

Q U A D R A N T S		BASALT CONC, 2							total
		VL	L	ML	M	HW	H	VW	
	1ST	0	0	1	3	3	2	0	9
	2ND	0	0	4	2	1	0	0	7
	3RD	0	0	3	5	0	1	0	9
	4TH	0	0	1	3	5	0	0	9
	total	0	0	9	13	9	3	0	34

C.4 INTERACTIONS

A large number of possible parameter interactions was investigated, both by plotting data and by computation of correlation coefficients, without finding any meaningful relationships. Among the trial interactions looked at were the following:

1. Basalt concentration vs density, quadrant by quadrant and overall.
2. Basalt concentration in one quadrant vs basalt concentration in another.
3. Density in one quadrant vs density in another.
4. Density in one quadrant vs basalt concentration in another.
5. Density vs distance along the simulator, quadrant by quadrant and overall.
6. Basalt concentration vs distance along the simulator, quadrant by quadrant and overall.

Some of the interactions above produced suggestive correlations, ie, correlation coefficients as large as 0.6. For example, one finds a suggestive correlation between basalt concentration and density for the run 4 data, using all 36 samples. However, no such correlation is evident for run 3. Moreover, when the individual quadrant data are plotted in the same way, none of the curves produced is like any other or like the overall curve. It was concluded that the appearance of correlation was accidental. Actually, the range of basalt concentration measured in these tests is too short to have an effect on packed density commensurate with the measured density range. Likewise, it is not clear how the deposited density could be a cause of, or generally correlate with, the local basalt concentration. It is probable that the two are independent, and responsive only to the feed ratio and to the local aerodynamic situation, the parameters governing which are not accessible in the present experimental configuration.

APPENDIX D
SAMPLE DATA SHEETS

Sheet ____ of ____

PNEUMATIC BACKFILL EMPLACEMENT
TEST DATA - FIRST SHEET

Test No: _____ Date: _____

General Purpose: _____

Test Operator(s): _____

Conditions: _____

Component Weights:	<u>Basalt</u>	<u>Bentonite</u>	<u>Simulator</u>
Initial	_____	_____	_____
Final	_____	_____	_____
Net	_____	_____	_____

Feeder Indices (initial): Basalt _____ Bentonite _____

Temperature _____ Barometric Pressure _____

Bleed Valve _____ Tape Record _____

Other Remarks on Test Conditions:

General Comments on Test Outcome:

Operator Signature: _____

Date: _____

HOMOGENIETY DATA - TEST SERIES _____

Sampling Position	Basalt Concentration, %				
	Sample 1	Sample 2	Sample 3	Mean	Std. Dev.
A5					
A6					
B1					
C1					
D1					
E1					
G1					
H1					
J1					
K1					
L1					
M1					
N1					
P1					
R1					
C4					
D4					
E4					
F4					
H4					
J4					
K4					
M4					
N4					
P4					
C3					
D3					
E3					
H3					

HOMOGENEITY DATA - TEST SERIES _____
(Continued)

Sampling Position	Basalt Concentration, %				
	Sample 1	Sample 2	Sample 3	Mean	Std. Dev.
J3	_____	_____	_____	_____	_____
K3	_____	_____	_____	_____	_____
M3	_____	_____	_____	_____	_____
N3	_____	_____	_____	_____	_____
P3	_____	_____	_____	_____	_____
C2	_____	_____	_____	_____	_____
D2	_____	_____	_____	_____	_____
E2	_____	_____	_____	_____	_____
H2	_____	_____	_____	_____	_____
J2	_____	_____	_____	_____	_____
K2	_____	_____	_____	_____	_____
M2	_____	_____	_____	_____	_____
N2	_____	_____	_____	_____	_____
P2	_____	_____	_____	_____	_____

APPENDIX E
Listing and Sample Output of Computer Program HIERARC2
(Written for the IBM PC)

15:48:32

02-03-1984

```

10 *          ***** PROGRAM HIERARC2.BAS *****
20 *
30 *WRITTEN BY J. M. MARKOWITZ          VERSION 2   DECEMBER 09, 1983
40 *                                     REVISED    FEBRUARY 03, 1984
50 *
60 *      HIERARC2 ANALYZES A THREE-LEVEL HIERARCHAL DESIGN OF ANY COMPLEX-
70 *      ITY AND PRINTS AS OUTPUT THE RESULTING ANOVA TABLE, THE INDIVIDUAL COMP-
80 *      ONENTS OF VARIANCE, THE OVERALL VARIANCE, AND (IN THE CASE OF NO MORE
90 *      THAN TWO BATCHES) A COMPUTED VALUE OF THE STUDENT'S T-STATISTIC FOR THE
100 *     DIFFERENCE BETWEEN THE BATCH MEANS. THE RIGHT TAIL PROBABILITY AREA
110 *     FOR THE T-VALUE AND THE APPROPRIATE DEGREES OF FREEDOM ARE ALSO PRINTED.
120 *     THE "EQUAL MEANS" HYPOTHESIS IS ASSESSED, BASED ON THE F-RATIOS FROM THE
130 *     ANOVA TABLE AND FROM THE T-VALUE. THE LATTER IS CALCULATED FROM THE
140 *     SQUARE ROOT OF THE BATCHES/SAMPLES F-RATIO. MANY OF THE INTERMEDIATE
150 *     STATISTICAL QUANTITIES OF POSSIBLE INTEREST ARE ALSO PRINTED.
160 *
170 *
180 *          ***** INPUT *****
190 *
200 *      DATA IS TO BE INPUT WITH DATA STATEMENTS STARTING WITH STATEMENT
210 *     NUMBER 7010 AS FOLLOWS:
220 *     STATEMENT 7010
230 *         NUMBER OF BATCHES (K)
240 *         NUMBER OF SAMPLES PER BATCH (L)
250 *         NUMBER OF SUB-SAMPLES (FOR ANALYSIS) PER SAMPLE (M)
260 *     STATEMENT 7020:
270 *         ALPHANUMERIC TITLE (50 CHARACTERS MAXIMUM), AND OPERATOR'S NAME.
280 *     STATEMENT 7030:
290 *         Y-OBSERVATIONS IN ORDER, IE, ASCENDING ORDER OF M WITHIN L
300 *         SAMPLES, ASCENDING ORDER OF L WITHIN K BATCHES, AND ASCENDING
310 *         ORDER OF K.
320 *
330 *      THERE MUST BE K*L*M OBSERVATIONS; OTHERWISE THE PROGRAM WILL ABORT
340 *     WITH AN ERROR MESSAGE. OTHER CASE DATA SHOULD FOLLOW THE SAME SEQUENCE
350 *     AS ABOVE; END EACH CASE WITH STATEMENT "DATA 999999". TERMINATE THE PRO-
360 *     GRAM WITH A STATEMENT "DATA 30000". IF THE PROGRAM ABORTS IN THE LAST
370 *     CASE WITH NO ERROR MESSAGE AND THE LAST ITEM IN THE OUTPUT "DATA" IS
380 *     30000, TWO OR MORE ITEMS OF DATA HAVE BEEN OMITTED.
390 *
400 *

```

```
410 *          ***** OTHER MATTERS *****
420 *
430 *   AMONG THE OUTPUT QUANTITIES WILL BE FOUND (FOR CASES WITH K = 2) A
440 *   BATCH-TO-BATCH COMPARISON OF MEAN, CRUDE SUM OF SQUARES, CORRECTION
350 *   FACTOR, CORRECTED SUM OF SQUARES, DIRECT ESTIMATE OF VARIANCE, AND SAMPLE
360 *   SUM. THE POOLED VARIANCE AND THE DIRECTLY CALCULATED T-VALUE FOR THE
450 *   DIFFERENCE BETWEEN MEANS ARE ALSO PRINTED. CAUTION; THE ABOVE QUANTITIES
380 *   ARE NOT USED IN THE SUBSEQUENT CALCULATION OF THE RIGHT TAIL PROBABILITY
460 *   VALUE OF THE T-DISTRIBUTION; INSTEAD, THE CORRESPONDING VALUES FROM THE
470 *   EARLIER ANOVA CALCULATION ARE USED, BECAUSE THEY, UNLIKE DIRECT BATCH-
480 *   TO-BATCH COMPARISON, TAKE INTO ACCOUNT THE HIERARCHAL NATURE OF THE BATCH
490 *   ANALYSIS, INCLUDING SAMPLING AND ANALYTICAL VARIANCE. LIKEWISE, THE
500 *   MEANS OF THE TWO BATCHES MUST BE ASSOCIATED WITH THE ANOVA CALCULATED
510 *   VALUE OF THE VARIANCE OF Y-BAR AND NOT WITH THE VARIANCE CALCULATED FOR
520 *   EACH BATCH OR WITH THE POOLED VARIANCE FROM THE DIRECT CALCULATION.
530 *
540 *
550 *          ** LIBRARY OF VARIABLES **
560 *
570 * K - NUMBER OF BATCHES
580 * L - NUMBER OF SAMPLES PER BATCH
590 * M - NUMBER OF SUB-SAMPLES (FOR ANALYSIS) PER SAMPLE
600 * J,I,H - RUNNING INDEXES ASSOCIATED RESPECTIVELY WITH K,L,M
610 * Y - DEPENDENT VARIABLE; Y(H,I,J) IS AN ITEM OF INPUT
620 * KX -DUMMY VARIABLE USED TO CHECK INPUT
630 * SM - SUBSAMPLE RUNNING SUM
640 * SQ - SUBSAMPLE RUNNING SUM OF SQUARES
650 * Ssq(I,J) - SUBSAMPLE SUM OF SQUARES WITHIN SAMPLES
660 * SSM(I,J) - SUBSAMPLE SUM WITHIN SAMPLES
670 * SBSQ - RUNNING SAMPLE SUM SQUARED WITHIN BATCHES; SAMPLE SUM OF SQUARES
680 * TOT - RUNNING TOTAL OF OBSERVATIONS, Y
690 * CSS - RUNNING TOTAL CRUDE SUM OF SQUARES
700 * CSS(J) - CRUDE SUM OF SQUARES FOR EACH BATCH = BSQ(J)
710 * BSM(J) - SAMPLE SUM WITHIN BATCHES
720 * BSQ(J) - SAMPLE SUM OF SQUARES WITHIN BATCHES
730 * SBSQ - RUNNING BETWEEN BATCHES SUM OF SQUARES; BATCH SUM OF SQUARES
740 * CF - CORRECTION FACTOR FOR ALL THE DATA
750 * CF(J) - CORRECTION FACTOR FOR EACH BATCH
760 * SY2 - CORRECTED SUM OF SQUARES FOR ALL THE DATA
770 * SY2(J) - CORRECTED SUM OF SQUARES FOR EACH BATCH
780 * ASQ - ANALYSIS (SUB-SAMPLE) SUM OF SQUARES
790 * TOT(J) - RUNNING OBSERVATION TOTAL WITHIN BATCHES, EQUALS BSM(J)
800 * CSS(J) - RUNNING CRUDE SUM OF SQUARES WITHIN BATCHES, EQUALS BSQ(J)
810 * NN(J) - MEAN OF EACH BATCH
820 * NN - OVERALL MEAN
830 * V(J) -ESTIMATE OF VARIANCE FOR EACH BATCH
840 * PV - POOLED ESTIMATE OF VARIANCE
850 * BV - ESTIMATE OF VARIANCE OF Y-BAR FROM ANOVA CALCULATION
860 * A - ANALYSIS MEAN SQUARE
870 * S - SAMPLE MEAN SQUARE
880 * B - BATCH MEAN SQUARE
890 * T - CALCULATED VALUE OF STUDENT'S T = TX
900 * E - INDEX OF CASE NUMBER
910 * N,P,Q,U,R,Y,Z - PARAMETERS USED IN RIGHT TAIL CALCULATION
920 * D - DEGREES OF FREEDOM (OVERALL)
930 *
```

```

940 '
950 '                                ** CALCULATION **
960 '
970 'INITIALIZE
980 OPTION BASE 1
990 DEFINT D, E, H-M
1000 DEFDBL S, B, C, A, P, V, T, N, X, Y, Z, U, R, F
1010 E = 0
1020 LPRINT: IF E = 0 GOTO 1050
1030 LPRINT TAB(32) "*****END OF CASE*****": LPRINT
1040 LPRINT CHR$(12)
1050 E = E + 1
1060 READ K
1070 IF K = 30000 GOTO 10000
1080 READ L, M
1090 IF E = 1 GOTO 1120
1100 ERASE BSM, TOT, CSS, NN, BBSQ, V, CF, SYZ
1110 ERASE Y, SSM, SSQ
1120 DIM BSM(K), TOT(K), CSS(K), NN(K), BBSQ(K), V(K), CF(K), SYZ(K)
1130 DIM Y(M, L), SSM(L, K), SSQ(L, K)
1140 READ TITLE$, OPERATOR$
1150 LPRINT
1160 LPRINT
1170 IF E > 1 GOTO 1210
1180 LPRINT CHR$(14); "HIERARCHAL DESIGN ANALYSIS"
1190 LPRINT
1200 LPRINT TIME$ TAB(65) DATE$
1210 LPRINT
1220 LPRINT CHR$(15); : LPRINT CHR$(14); "CASE "; E; ", "; TITLE$ TAB(55) OPERATOR$
1230 LPRINT
1240 LPRINT CHR$(18);
1250 LPRINT
1260 LPRINT
1270 LPRINT
1280 CSS = 0: SBSQ = 0
1290 TOT = 0: BBSQ = 0: CF = 0
1300 LPRINT "DATA: K = "; K, "L = "; L, "M = "; M : LPRINT
1310 '
1320 FOR J = 1 TO K
1330 FOR I = 1 TO L
1340 SM = 0
1350 SQ = 0
1360 '
1370 '
1380 'ACCUMULATE SUMS AND SUMS OF SQUARES
1390 FOR H = 1 TO M
1400 READ Y(H, I)
1410 PRINT
1420 LPRINT Y(H, I);
1430 SM = SM + Y(H, I)
1440 SQ = SQ + Y(H, I)^2

```

```

1450 NEXT H
1460 SSM(I,J) = SSM(I,J) + SM
1470 SSQ(I,J) = SSQ(I,J) + SQ
1480 SBSQ = SBSQ + SSM(I,J)^2
1490 TOT = TOT + SM
1500 CSS = CSS + SQ
1510 BSM(J) = BSM(J) + SSM(I,J)
1520 BSQ(J) = BSQ(J) + SSQ(I,J)
1530 NEXT I
1540 BBSQ = BBSQ + BSM(J)^2
1550 CSS(J) = BSQ(J)
1560 NEXT J
1570 CF = TOT^2/(K*L*M)
1580 SY2 = CSS - CF
1590 BBSQ = (BBSQ/(L*M)) - CF
1600 SBSQ = (SBSQ/M) - BBSQ - CF
1610 ASQ = SY2 - BBSQ - SBSQ
1620 LPRINT
1630 LPRINT
1640 READ KX!
1650 IF KX! = 999999! GOTO 1680
1660 LPRINT "PROGRAM ABORTS BECAUSE NUMBER OF Y-OBSERVATIONS <> K*L*M"
1670 GOTO 10000
1680 "REFINE AND PRINT OUT RESULTS.
1690 LPRINT "THE CRUDE SUM OF SQUARES IS";CSNG (CSS)
1700 LPRINT "THE CORRECTION FACTOR IS";CSNG (CF)
1710 LPRINT
1720 LPRINT
1730 LPRINT "ANOVA:"
1740 LPRINT "-----"
1750 LPRINT
1760 LET DFB = (K - 1)
1770 LET DFS = K*(L - 1)
1780 LET DFA = K*L*(M - 1)
1790 LPRINT "SOURCE", "SSQ", "DF", "MEAN SQ", "F-RATIO"
1800 LPRINT "-----", "-----", "-----", "-----", "-----"
1810 LPRINT
1820 LET B = BBSQ/DFB
1830 LET S = SBSQ/DFS
1840 LET A = ASQ/DFA
1850 LPRINT "SY2",CSNG (SY2),K*L*M -1
1860 LPRINT "B SSQ",CSNG (BBSQ),DFB,CSNG (B)
1870 LPRINT "S SSQ",CSNG (SBSQ),DFS,CSNG (S),"B/S: ";CSNG (B/S)
1880 LPRINT "A SSQ",CSNG (ASQ),DFA,CSNG (A),"S/A: ";CSNG (S/A)
1890 LPRINT
1900 LPRINT
1910 LPRINT "ESTIMATE OF ANALYTICAL VARIANCE = ";CSNG (A)
1920 LPRINT "ESTIMATE OF WITHIN BATCH VARIANCE = ";(CSNG (S) - CSNG (A))/M
1930 LPRINT "ESTIMATE OF BETWEEN BATCH VARIANCE = ";(CSNG (B) - CSNG (S))/(M*L)
1940 IF (A>0) AND ((S-A)/M)>0) AND ((B-S)/(M*L))>0) GOTO 1990
1950

```

```

1960 LPRINT "      (NOTE:  NEGATIVE ESTIMATES OF VARIANCE COMPONENTS WILL OCCASIO
NALLY
1970 LPRINT "      OCCUR IN HIERARCHAL DESIGN CALCULATIONS.  THEY ARE, OF COURSE
1980 LPRINT "      APHYSICAL, AND IN SUCH CASES THE ESTIMATE IS TAKEN TO BE ZERO.
)"
1990 LPRINT
2000 IF ((B - S)/(M*L) > (S - A)/M) AND ((B - S)/(M*L) > A) GOTO 2030
2010 IF ((S - A)/M > (B - S)/(M*L)) AND ((S - A)/M > A) GOTO 2030
2020 IF (A > (S - A)/M) AND (A > (B - S)/(M*L)) GOTO 2070
2030 LPRINT "THE DOMINANT VARIABILITY IS THAT BETWEEN BATCHES."
2040 GOTO 2080
2050 LPRINT "THE DOMINANT VARIABILITY IS THAT WITHIN BATCHES (SAMPLING)."

```

```

2470 LPRINT "CRUDE SUM OF SQUARES" TAB(40) CSNG (CSS(1)) TAB(55) CSNG (CSS(2))
2480 LPRINT "CORRECTION FACTOR" TAB(40) CSNG (CF(1)) TAB(55) CSNG (CF(2))
2490 LPRINT "CORR. SUM OF SQUARES " TAB(40) CSNG (SY2(1)) TAB(55) CSNG (SY2(2))
2500 LPRINT "ESTIMATE OF VARIANCE" TAB(40) CSNG (V(1)) TAB(55) CSNG (V(2))
2510 LPRINT "SAMPLE SUM" TAB(40) CSNG (BSM(1)) TAB(55) CSNG (BSM(2))
2520 LPRINT
2530 LPRINT
2540 LPRINT "THE POOLED VARIANCE IS";CSNG (PV)
2550 LPRINT "THE DIRECTLY CALCULATED T-VALUE IS ";CSNG (T);"WITH";(K&L&M -2);"DE
GREES OF FREEDOM."
2560 LET T = SQR (B/S); LET TX = T
2570 LPRINT "THE T-VALUE CALCULATED FROM F-RATIO B/S IS ";CSNG (T);"WITH";DFS;"D
EGREES OF FREEDOM."
2580 '
2590 '
2600 'NOW WE COMPUTE THE RIGHT TAIL VALUE OF THE T-DISTRIBUTION FOR THE
2610 'CALCULATED T-VALUE AND THE GIVEN DEGREES OF FREEDOM USING THE
2620 'ALGORITHM FROM THE IBM SET, NO. 57.
2630 D = DFS
2640 LPRINT
2650 X = 1
2660 Y = 1
2670 T = T*T
2680 'COMPUTE USING INVERSE FOR SMALL T-VALUES
2690 IF T < 1 THEN 2740
2700 U=Y
2710 R=D
2720 Z = T .
2730 GOTO 2770
2740 U=D
2750 R=Y
2760 Z=1/T
2770 N=2/9/U
2780 P=2/9/R
2790 'COMPUTE USING APPROXIMATION FORMULAS
2800 Q=ABS((1-P)*Z^(1/3)-1+N)/SQR(P*Z^(2/3)+N)
2810 IF R<4 THEN 2850
2820 X = .25/(1+Q*(.196854+Q*(.115194+Q*(.000344+Q*.019527))))^4
2830 X=INT(X*100000!+.5)/100000!
2840 GOTO 2880
2850 Q=Q*(1+.08*Q^4/R^3)
2860 GOTO 2820
2870 LPRINT
2880 LPRINT "BASED ON THE LATTER VALUE OF T AND ITS ASSOCIATED DEGREES OF FREEDO
M, THE RIGHT TAIL PROBABILITY VALUE OF THE T-DISTRIBUTION IS ";X
2890 LPRINT

```


7300 DATA 2,18,3
7310 DATA SERIES 4 HOMOGENEITY BACK VS FRONT, MARKOWITZ
7320 DATA 80.19,75.08,77.89,73.64,76.31,82.78,83.56,84.58,85.09
7330 DATA 80.37,78.55,78.19,68.84,66.15,66.62,73.85,83.44,76.11
7340 DATA 73.12,81.41,75.91,73.22,72.37,70.50,69.42,72.85,64.45
7350 DATA 75.42,69.83,69.59,76.77,71.57,78.12,74.42,71.64,71.50
7360 DATA 73.77,74.58,76.94,84.00,85.05,80.79,78.02,79.61,78.59
7370 DATA 75.84,70.35,77.31
7380 DATA 78.29,75.08,78.40,72.29,72.29,77.28,74.63,76.53,76.48
7390 DATA 68.87,69.58,69.35,65.23,68.95,68.95,76.62,72.73,74.19
7400 DATA 88.42,84.07,87.61,81.86,80.59,82.75,75.42,78.89,74.17
7410 DATA 83.22,86.67,76.42,67.51,69.45,68.38,69.49,68.95,65.10
7420 DATA 73.46,70.54,69.52,78.49,74.92,73.04,75.30,77.30,69.82
7430 DATA 74.48,69.92,82.37
7440 DATA 999999
7450 DATA 2,18,3
7460 DATA SERIES 3 HOMOGENEITY TOP VS BOTTOM, MARKOWITZ
7470 DATA 83.7,81.87,83.43,75.81,82.3,88.06,69.98,75.8,69.74
7480 DATA 81.38,74.77,73.61,69.79,69.93,73.95,60.34,59.66,64.56
7490 DATA 71.66,76.5,76.12,67.05,71.38,69.54,72.7,74.96,76.67
7500 DATA 71.71,70.60,77.35,79.76,78.3,77.55,67.04,69.65,66.15
7510 DATA 75.9,74.18,79.72,70.14,76.82,66.75,60.70,62.15,61.97
7520 DATA 75.33,80.04,74.09,69.3,71.04,73.27,76.51,75.1,75.89
7530 DATA 86.83,85.54,77.37,74.34,70.22,68.54,60.76,62.26,61.38
7540 DATA 53.49,50.45,51.6,73.42,72.93,71.69,86.91,91.52,82.24
7550 DATA 79.19,85.10,82.62,78.45,80.06,81.89,74.86,77.96,82.28
7560 DATA 77.07,75.52,75.17,76.03,76.79,76.03,75.12,79.45,79.3
7570 DATA 71.26,76.25,69.78,71.51,71.04,71.94,80.23,81.93,81.08
7580 DATA 74.35,73.71,76.73,74.71,79.19,77.94,76.28,75.72,76.29
7590 DATA 999999
7600 DATA 2,18,3
7610 DATA SERIES 3 HOMOGENEITY RIGHT VS LEFT, MARKOWITZ
7620 DATA 83.7,81.87,83.43,75.81,82.3,88.06,69.98,75.8,69.74
7630 DATA 81.38,74.77,73.61,69.79,69.93,73.95,60.34,59.66,64.56
7640 DATA 71.66,76.5,76.12,67.05,71.38,69.54,72.70,74.96,76.67
7650 DATA 77.07,75.52,75.17,76.03,76.79,76.03,75.12,79.45,79.30
7660 DATA 71.26,76.25,69.78,71.51,71.04,71.94,80.23,81.93,81.08
7670 DATA 74.35,73.71,76.73,74.71,79.19,77.94,76.28,75.72,76.29
7680 DATA 71.71,70.60,77.35,79.76,78.30,77.55,67.04,69.65,66.15
7690 DATA 75.90,74.18,79.72,70.14,76.82,66.75,60.70,62.15,61.97
7700 DATA 75.33,80.04,74.09,69.30,71.04,73.27,76.51,75.10,75.89
7710 DATA 86.83,85.54,77.37,74.34,70.22,68.54,60.76,62.26,61.38
7720 DATA 53.49,50.45,51.60,73.42,72.93,71.69,86.91,91.52,82.24
7730 DATA 79.19,85.10,82.62,78.45,80.06,81.89,74.86,77.96,82.28
7740 DATA 999999

7750 DATA 2,18,3
7760 DATA SERIES 3 HOMOGENEITY BACK VS FRONT, MARKOWITZ
7770 DATA 83.70,81.87,83.43,71.71,70.60,77.33,86.83,85.54,77.37
7780 DATA 77.07,73.32,73.17,73.81,82.30,88.06,79.76,78.30,77.53
7790 DATA 74.34,70.22,68.54,76.03,76.79,76.03,69.98,73.80,69.74
7800 DATA 67.04,69.65,66.13,60.76,62.26,61.38,73.12,79.45,79.30
7810 DATA 81.38,74.77,73.61,73.90,74.18,79.72,53.49,50.45,51.60
7820 DATA 71.26,76.25,69.78,73.42,72.93,71.69,71.51,71.04,71.94
7830 DATA 69.79,69.93,73.93,70.14,76.82,66.75,60.34,59.66,64.36
7840 DATA 60.70,62.15,61.97,86.91,91.52,82.24,80.23,81.93,81.08
7850 DATA 71.66,76.50,76.12,73.33,80.04,74.09,79.19,85.10,82.62
7860 DATA 74.33,73.71,76.73,67.05,71.38,69.54,69.30,71.04,73.27
7870 DATA 78.45,80.06,81.89,74.71,79.19,77.94,72.70,74.96,76.67
7880 DATA 76.51,73.10,73.89,74.86,77.96,82.28,76.28,73.72,76.29
7890 DATA 999999
7900 DATA 2,18,1
7910 DATA SERIES 4 DENSITIES TOP VS BOTTOM, MARKOWITZ
7920 DATA 1.61,1.66,1.57,1.63,1.68,1.62,1.77,1.66,1.71
7930 DATA 1.59,1.56,1.64,1.59,1.64,1.57,1.61,1.66,1.63
7940 DATA 1.60,1.47,1.42,1.43,1.51,1.66,1.52,1.53,1.60
7950 DATA 1.59,1.43,1.34,1.39,1.43,1.50,1.53,1.42,1.51,999999
7960 DATA 2,18,1
7970 DATA SERIES 4 DENSITIES RIGHT VS LEFT, MARKOWITZ
7980 DATA 1.61,1.66,1.57,1.63,1.68,1.62,1.77,1.66,1.71
7990 DATA 1.59,1.43,1.34,1.39,1.43,1.50,1.53,1.42,1.51
8000 DATA 1.59,1.56,1.64,1.59,1.64,1.57,1.61,1.66,1.63
8010 DATA 1.60,1.47,1.42,1.43,1.51,1.66,1.52,1.53,1.60,999999
8020 DATA 2,16,1
8030 DATA SERIES 4 DENSITIES FRONT VS BACK, MARKOWITZ
8040 DATA 1.61,1.59,1.60,1.59,1.66,1.56,1.47,1.43
8050 DATA 1.57,1.64,1.42,1.34,1.63,1.59,1.43,1.34
8060 DATA 1.71,1.63,1.60,1.51,1.42,1.53,1.66,1.66
8070 DATA 1.77,1.61,1.52,1.53,1.50,1.66,1.62,1.57,999999
8080 DATA 2,18,1
8090 DATA SERIES 3 DENSITIES TOP VS BOTTOM, MARKOWITZ
8100 DATA 1.60,1.66,1.66,1.62,1.82,1.63,1.62,1.57,1.64
8110 DATA 1.73,1.77,1.62,1.60,1.68,1.58,1.59,1.62,1.66
8120 DATA 1.65,1.61,1.47,1.40,1.34,1.48,1.53,1.46,1.43
8130 DATA 1.59,1.51,1.53,1.48,1.32,1.37,1.39,1.33,1.37,999999
8140 DATA 2,18,1
8150 DATA SERIES 3 DENSITIES RIGHT VS LEFT, MARKOWITZ
8160 DATA 1.60,1.66,1.66,1.62,1.82,1.63,1.62,1.57,1.64
8170 DATA 1.59,1.51,1.53,1.48,1.32,1.37,1.39,1.33,1.37
8180 DATA 1.73,1.77,1.62,1.60,1.68,1.58,1.59,1.62,1.66
8190 DATA 1.65,1.61,1.47,1.40,1.34,1.48,1.53,1.46,1.43,999999
8200 DATA 2,16,1
8210 DATA SERIES 3 DENSITIES FRONT VS BACK, MARKOWITZ
8220 DATA 1.59,1.60,1.73,1.63,1.66,1.77,1.61,1.51
8230 DATA 1.66,1.62,1.47,1.53,1.62,1.60,1.40,1.48
8240 DATA 1.63,1.58,1.48,1.37,1.62,1.59,1.53,1.39
8250 DATA 1.57,1.62,1.46,1.33,1.64,1.66,1.43,1.37,999999,30000

WTSD-TME-030
DRAFT

10000 LPRINT : LPRINT : LPRINT TAB(30) "***** END OF PROGRAM *****"
10010 END

***** END OF PROGRAM *****

HIERARCHAL DESIGN ANALYSIS

13:12:48

02-03-1984

CASE 1 , SERIES 4 HOMOGENEITY TOP VS BOTTOM

MARKOWITZ

DATA: K = 2 L = 18 M = 3

80.19	75.08	77.89	73.85	83.44	76.11	69.42	72.85	64.45	84	85.05
80.79	84.5	77.61	80.39	75.3	77.3	69.82	75.42	78.89	74.17	88.42
84.07	87.61	78.29	75.08	78.4	73.64	76.31	82.78	73.12	81.41	75.91
73.42	69.83	69.59	78.02	79.61	78.59	81.97	72.84	78.82	74.48	69.92
82.37	83.22	86.67	76.42	81.86	80.59	82.75	72.29	72.29	77.28	83.56
84.58	85.09	73.22	72.37	70.5	76.77	71.57	78.12	75.84	70.35	77.31
75.26	72.45	69.34	78.49	74.92	73.04	67.51	69.45	68.38	76.62	72.73
74.19	74.63	76.53	76.48	80.37	78.53	78.19	68.84	66.15	66.62	74.42
71.64	71.5	73.77	74.58	76.94	66.43	64.5	66.17	73.46	70.54	69.52
69.49	68.95	65.1	65.23	68.95	68.95	68.87	69.58	69.35		

THE CRUDE SUM OF SQUARES IS 614225.4
THE CORRECTION FACTOR IS 610837.1

ANOVA:

SOURCE	SSQ	DF	MEAN SQ	F-RATIO
SY2	3368.225	107		
B SSQ	677.1713	1	677.1713	
S SSQ	2049.852	34	60.28977	B/S: 11.23194
A SSQ	641.2017	72	8.905579	S/A: 6.769888

ESTIMATE OF ANALYTICAL VARIANCE = 8.905579
ESTIMATE OF WITHIN BATCH VARIANCE = 17.12806
ESTIMATE OF BETWEEN BATCH VARIANCE = 11.42373

THE DOMINANT VARIABILITY IS THAT WITHIN BATCHES (SAMPLING).

FROM AN (UPPER 5%) F TABLE, ENTER $F(1, 34) = 4.13$
IF F-RATIO B/S IS LESS THAN THE TABULAR ENTRY ABOVE, THE
DIFFERENCE BETWEEN BATCHES IS NOT SIGNIFICANT; AND CONVERSELY.

FROM AN (UPPER 5%) F TABLE, ENTER $F(34, 72) = 2.01$
IF F-RATIO S/A IS LESS THAN THE TABULAR ENTRY ABOVE, THE
DIFFERENCE BETWEEN SAMPLES IS NOT SIGNIFICANT; AND CONVERSELY.

THE OVERALL AVERAGE = 75.20695
STD. DEV. OF A SINGLE MEASUREMENT IS 5.610592
STANDARD ERROR OF THE MEAN IS .5398795

PARAMETER	BATCH 1	BATCH 2
MEAN	77.71093	72.70296
CRUDE SUM OF SQUARES	327519.5	286705.9
CORRECTION FACTOR	326105.4	285429
CORR. SUM OF SQUARES	1414.126	1276.912
ESTIMATE OF VARIANCE	26.68162	24.09268
SAMPLE SUM	4196.39	3925.96

THE POOLED VARIANCE IS 25.38715
THE DIRECTLY CALCULATED T-VALUE IS 3.164593 WITH 106 DEGREES OF FREEDOM.
THE T-VALUE CALCULATED FROM F-RATIO B/S IS 3.351409 WITH 34 DEGREES OF FREEDOM.

BASED ON THE LATTER VALUE OF T AND ITS ASSOCIATED DEGREES OF FREEDOM, THE RIGHT
TAIL PROBABILITY VALUE OF THE T-DISTRIBUTION IS .00116

GIVEN THAT THE MEANS ARE EQUAL, A T-VALUE AS LARGE AS 3.351409
IS THEREFORE A RARE EVENT (TWO-TAILED PROBABILITY < .05). WE CONCLUDE THAT THE
DATA CONTRADICT THE HYPOTHESIS THAT THE BATCH MEANS ARE EQUAL.
THE DIFFERENCE BETWEEN MEANS IS SIGNIFICANT.

*****END OF CASE*****